

**PART II      DETAILED REPORT ON  
THE ZHAMAN-AIBAT AREA**



## Part II Detailed Report on the Zhaman-Aibat Area

### Chapter 1 Previous Survey Data

#### 1-1 Mining Activities in the Zhezkazgan Area

The Zhaman-Aibat Area is located 180 km southeast of Zhezkazgan. The Zhezkazgan area has long been known for its production of copper ore and copper. Historical progress of the Zhezkazgan mine and smelting plant is shown below;

- 1771; The Russian geographer Captain Richkov described the Zhezkazgan deposit in his "Notes on Antiquities".
- 1847; The Zhezkazgan copper deposit and the Baikonur coal-mines were purchased by Russian merchants and industrialists, later they became British concessions.
- 1928; The Atbasar Non-Ferrous Metals Trust was established and incorporated the Karsakpai Combine which amalgamated the copper smelting plant, the Baikonur coal mine, the Zhezkazgan copper mine and the Kurgasyu mine.
- 1929-41; Kanysh Satpaev supervised the prospecting of the Zhezkazgan copper deposit.
- 1936; Decided to construct the Zhezkazgan copper smelting plant.
- 1937; Connected with nationwide railway network.
- 1943; Organized the Zhezkazgan Combine which comprised 17 mines, 3 open pits, the Karsakpai copper smelting plant, Baikonur coal mine, etc.
- 1945-55; Built new mines and put into operation; Petre-Center, Pokro, Nos.3,42,44,45,51; the open pits Karpiev, Nikol, Krestov, Moly Zlatoust and an ore dressing factory.
- 1958; An excavator, electric dump-truck and four-puncher boring machine were introduced to operate in underground mine No.45.
- 1963,1965; Commenced the first cycle and the second cycle of No.2 Ore-Dressing facility operation.
- 1965-67; Commenced operation of Giant Mines No.55 and No.57.
- 1975; Commenced operation of No.65 Mine.
- 1977; Commenced operation and production of the whole copper-smelting plant.
- 1985; Commenced operation of No.67 Mine. Reorganized the Satpaev Zhezkazgan Mining Smelting Combine into the Satpaev Scientific and Production Management, Zhezkazgantsvetment.
- 1995; 4 mines (1 open-pit mine, 3 underground mines) are being operated and 1 mine is under development. 2 ore dressing plants and 1 copper smelting plant are also being operated. The total annual production of electrolytic copper is approximately 200,000 tons.

## 1-2 Geological Surveys

Kanysh I. Satpayev paid special attention to issues of metallogeny and stratigraphy of the Zhezkazgan Area, and systematic geological works started in the 1920's. These works resulted in commercial estimation of the Zhezkazgan area in the 1930's and this area was recognized as one of the most important mining areas in Kazakhstan.

In the 1940's several important exploration works were done by regular geological mapping methods. In 1953, the Taskura deposit was explored by drilling which confirmed mineralization rich in copper located close to the surface. Since 1959, the Zhezkazgan Expedition Party has carried out exploration drillings for copper deposits in the Zhezkazgan Area. From 1959 to 1964, exploration parties drilled in the Zhaman-Aibat Area and confirmed copper mineralization at the depth of 400 - 700m beneath the surface. Its thickness was estimated as 0.4 - 1.0m with copper grade of 1.16 - 1.30%. During the period from 1981 to 1984, the exploration by the Zhezkazgan Exploration Expedition Party resulted in the detection of commercial grade copper and copper-lead mineralization at the depth of 615m - 700m.

Drilling statistics from 1981 to December 1996 are summarized in Table 2-1-1 and the location map of drill holes are shown in Fig.2-1-1. These drill holes are divided into five groups on the basis of exploration stages and correlate to the following ore reserve categories: drilling for overall prospecting is correlated to P1 and P2 categories; drilling for detailed prospecting, preliminary estimation and preliminary survey are correlated to C2, C1, A and/or B categories, respectively. Beside these, drillholes for prospecting are considered to be a kind of scout drilling in the ordinary exploration strategy.

All mineralized cores have been used for various kinds of chemical assay and ore dressing test. Only small pieces of mineralized core of each drill hole have been retained as preserved samples.



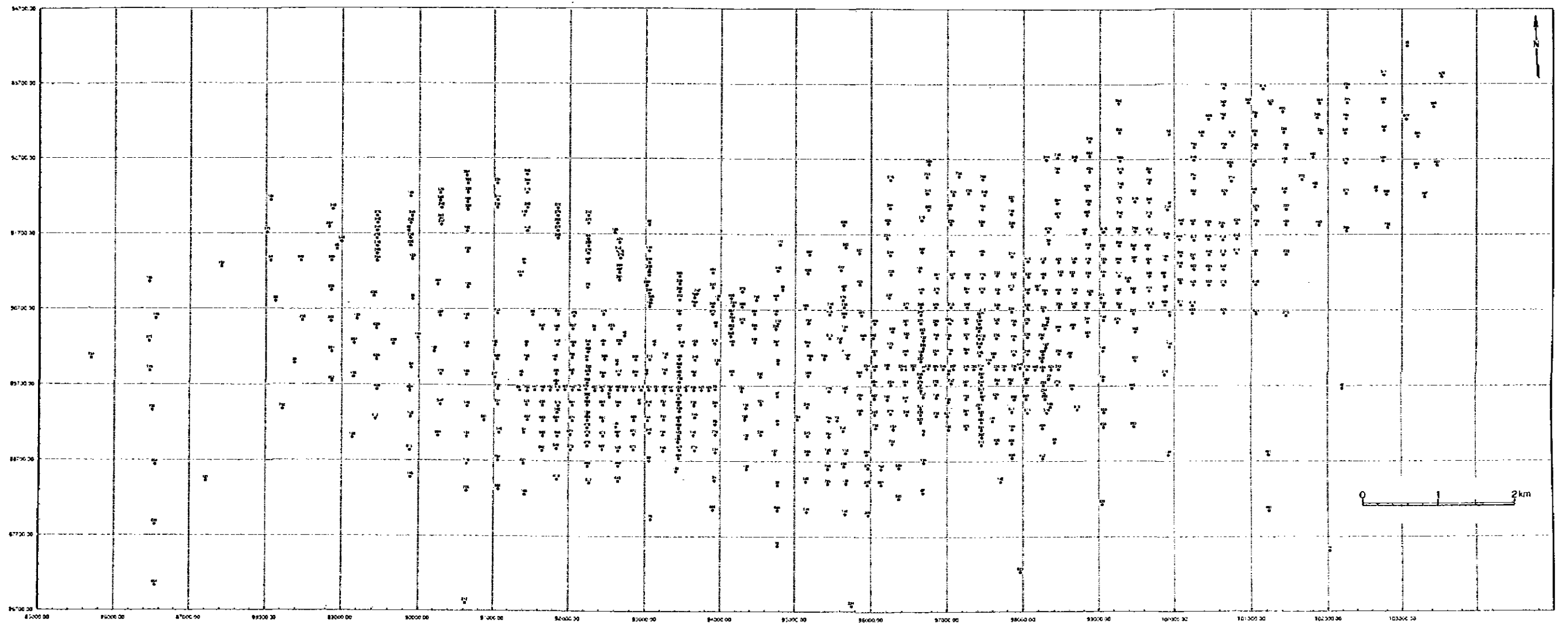


Fig. 2-1-1 Location Map of Drill Holes in the Zhaman-Aibat Ore Deposit



Table 2-1-1. Drilling Statistics in the Zhaman-Aibat Area

Year	Total Prospecting, P1,P2		Detailed Prospecting, C2		Prospecting Estimation, C1	
	Nos of drill	Total Length	Nos of drill	Total Length	Nos of drill	Total Length
	(TD)	m	(TD)	m	(TD)	m
1981	2	1,760.0				
1982	14	11,743.6				
1983	19	16,110.1				
1984			25	20,656.9		
1985			37	30,869.7		
1986			26	20,297.3		
1987			2	1,667.2	26	7
1988					57	
1989						
1990						
1991						
1992						
1993						
1994						
1995						
1996						
Subtotal	35	0	90	0	83	7
Total	35	29,613.7	90	73,491.1	90	59,728.5

Year	Preliminary A & B (include, C1)		Prospecting		Total	
	Nos of drill	Total Length	Nos of drill	Total Length	Nos of drill	Total Length
	(TD)	m	(TD)	m	(TD)	m
1981					2	0
1982					14	0
1983					19	0
1984					25	0
1985					37	0
1986					26	0
1987					28	7
1988	85	50			142	50
1989	160	81	3	2,465.8	163	81
1990	95	25	16	13,634.6	111	25
1991	94	8	9	8,744.5	103	8
1992	56		7	6,382.8	63	0
1993	49				49	0
1994	24		2	1,880.0	26	0
1995	17				17	
1996	10				10	
Subtotal	590	164	37	0	835	171
Total	754	442,626.4	37	33,107.7	1006	638,587.4



### 1-3 Geochemical Explorations

Previous geochemical studies of the Zhaman-Aibat Area are given in Table 2-1-2.

The geochemical surveys (1981 to 1984, and 1987 to 1990) have resulted in delineating mono-element and complex haloes of chemical elements, forming four large halo areas, namely : Taskura, Zhaman-Aibat, Azat and Zhatyka.

The Taskura area (Cu is up to 0.8%, Ag is up to 0.004%, Pb is up to 0.025%, Ba is up to 8%) in its southeastern part exactly coincides with the Taskura copper deposit, localized in the sediments of the Kengir Formation. Its northwestern part is probably shaped as a scattering flow.

The Zhaman-Aibat Area (Cu is up to 0.03%, Ag is up to 0.00015%, Ba is up to 0.2%, Pb is up to 0.005%) is associated with deeply occurring mineralization (it is possible that haloes were injected from underneath along the zone of sub-latitudinal faults, supposed to be located here).

The Azal and the Zhatyka halo areas are confined to the central part of the Azat anticline and the Zhatyka halo area, respectively.

Table 2-1-2 List of Previous Geochemical Explorations  
in the Zhaman-Aibat Ore Deposit

Index	Organization	Survey year	Scale Network (m)
1	AGPhE, Stroiteleva A.	1954	1:200,000
2	DGPhE, Skalskii N.	1959	1:50,000
3	DGPhE, Skalskii N.	1960	1:50,000 500x50
4	DGPhE, Stefankevich Z.	1961	1:50,000 500x50
5	DGRE, Schuvatov T	1981-1984	1:50,000 500x50
6	DGRE, Scheripov A.	1987-1990	1:50,000 500x100

DGPhE-Zhezkazgan Geophysical Exploration Expedition  
 DGRE -Zhezkazgan Geological Exploration Expedition  
 AGPhE-Atasu Geophysical Expedition

#### 1-4 Geophysical Explorations

The previous geophysical surveys of the Zhaman-Aibat Area are given in Tables 2-1-3, 2-1-4, 2-1-5 and 2-1-6.

Geophysical studies of the area have been carried out since the 1950's. Areal magnetic surveys were completed in 1955 to 1996 at the scale of 1:50,000 and 1:100,000. They have resulted in a general understanding of the magnetic field in the area, and have assisted in evaluating prospects of finding iron ore related to ultrabasic bodies along deep seated faults.

The first ground survey was carried out by the Atasu Expedition (1954) in a small region (6km<sup>2</sup>), located in the western part of the area. The survey utilized electric methods (Electrical profiling, VES, etc.) and was targeted at prospecting for underground water. However, no positive results were obtained.

A 1:200,000 scale gravity survey was carried out by Zhezkazgan Geophysical Exploration Expedition in 1957. It spotted a large positive anomaly in the Zhaman-Aibat Area. These were however no geological interpretations given at that time.

Geophysical surveys at 1:50,000 scale were carried out by the Zhezkazgan Geophysical Exploration Expedition in 1959 to 1960 within the Zhaman-Aibat Area. These surveys included gravity, magnetic, electric survey of VES method and geochemical surveys. This work resulted in delineating the Zhaman-Aibat anticlinal structure (based on gravity and magnetic survey), and was handed over to the Zhezkazgan Geological Exploration Expedition for further proving of Zhezkazgan type copper mineralization by drilling. Test drilling was carried out in 1962 to 1964. Drilling however did not fully penetrate the structure (4-drillholes, 1925m). That work resulted in determining 0.4 - 1m intervals, by the drillings No. Y-3, Y-4 and Y-26, at the depth of 400 - 700m in grey sandstone within the productive rock mass, with the content of copper 0.4-1.16%. However the authors concluded a negative assessment of copper in the study area.

Between 1964 and 1974, the Zhezkazgan Depression was systematically studied by seismic survey MOV (Seismic reflection), in order to study the structure of the Upper Paleozoic rock masses and to delineate prospective oil and gas structures. Results in the form of maps of isodepth of reflecting horizons have shown an increase in thickness of the Carboniferous sediment in the eastern part of the Zhezkazgan-Sarysu depression close to the flanks (Faskura-Tasbulack trough). A number of anticlinal structures have been delineated which are prospective for oil and gas.

At the same time, a 1:50,000 gravity survey was carried out in part of the area in order to assist the interpretation of the seismic survey. A number of local positive gravity anomalies with 1 to 2 mgals amplitude as well as uplifts of the R2, R2', R3 horizon depth contours, outlining positions of subsidiary anticlines (Azat, Zhaman-Aibat) have been delineated within the huge structure.

Based on analysis of both geophysical and geological data collected by the Zhezkazgan Geological Exploration Expedition in 1980, a program of study and prospecting for copper in the Zhezkazgan-Sarysu depression was formulated. The Zhaman-Aibat anticline structure was included as a first priority structure. In compliance with that program, 1:50,000 scale geophysical surveys were carried out in the area of the Zhaman-Aibat structure from 1981 to 1984 and from 1987 to 1990. Surveys included gravity, magnetic, electric of VES, IP and ZSB (TEM) methods,

geochemical and shallow scout drilling. From 1983 to 1986, and 1990 to 1992 detailed seismic MOGT (CDP) survey were conducted in combination with electric surveys of ZSB (TEM) with spacing of 0.8 to 2 km.

Results of these surveys, made it possible to compile uniform maps of geophysical and geochemical fields covering the entire described area at the scales of 1:50,000 and 1:100,000 and to obtain valuable information on the deep structure of the territory, the structural position of the Zhaman-Aibat Deposit and possible directions of further prospecting and exploration works. It has been concluded that ore bodies and mineralization zones are located mostly on the flanks of local anticline structures and somehow frame them. This finding has made it possible to locate probable positions of ore zones not yet penetrated by drilling within Zhaman-Aibat and Azat structures and to place prospecting and exploration drillholes accordingly.

A magnetic map makes it possible to conclude that characteristics of the magnetic field are determined mostly by lithological irregularities in the crystalline basement. Quite intensive anomalies have been delineated in the eastern flank zone of the area, that are associated with magnetite containing sandstone of Taskuduk Formation. The rocks of this Formation however, do not cause any considerable anomaly in the Zhaman-Aibat Area, because they occur at considerable depths and laboratory measurements did not show any appreciable increase in magnetic susceptibility of the samples.

Based on analysis of electric survey of TEM data together with gravity data, the Kazybek area has been delineated on the south-eastern flank of the Zhaman-Aibat Deposits (9km<sup>2</sup>), where 6 wells are recommended to be drilled.

Borehole logging has been widely applied in the prospecting with the following objectives: to classify the cross section lithologically, to select intervals of mineralization and to estimate their thickness (IP, gamma ray) and to estimate the content of minerals (Roengeno-radiometric logging).

Table 2-1-3 Previous Magnetic Surveys in the Zhaman-Albat Area

No.	Organization	Year	System	Scale Network (m)	Accuracy mT
1	ZGT, Kukin G.	1952	Aeromagnetic Survey AEM-49	1:100,000	+/- 29
2	DGPHE, Stroitelova L.	1954	Aeromagnetic Survey M-2	1:200,000 1000x200 2000x4000	+/- 10-15
3	ZGT, Zavyalova L.	1955	Aeromagnetic Survey AEM-49	1:500,000	+/- 30
4	DGPHE, Stefankovich Z.	1961	Aeromagnetic Survey M-2	1:50,000 500x100	+/- 9.7
5	XGT, Sargashev Y.	1960	Aeromagnetic S. ASGM-25, ASG-45	1:100,000	+/- 25
6	DGPHE, Skalskii N.	1960	Ground survey M-2	1:50,000 500x50	+/- 11-14
7	DGRE, Kogal S.	1976-78	Ground survey MMS-1	1:50,000 500x10	+/- 11-14
9	DGRE, Shuvatov Y.	1984	Ground survey MKA-201	1:50,000 500x50	+/- 6
10	DGRE, Scharipov A.	1987-90	Ground survey MNP-203	1:50,000 500x100	+/- 3

ZGT - Western Geophysical Trust, KGT - Kazakh Geophysical Trust  
 DGPHE - ZHEZKAZGAN Geophysical Exploration Expedition  
 DGRE - ZHEZKAZGAN Geological Exploration Expedition

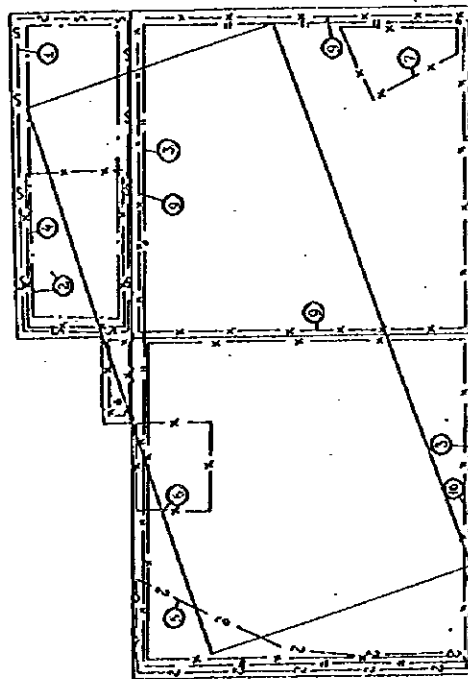


Table 2-1-4 Previous Gravity Surveys in the Zhaman-Albat Area

No	Organization	Survey Year	Grimmeter	Scale Network (km)	Accuracy (mgals)
3	DGPHE, Loskutov A.	1957	SK-3	1:200,000 4x1	+/- 0.50
4	DGPHE, Skalskii N.	1959	GAK-3M GAK-4M	1:50,000 0.5x0.5	+/- 0.21
5	DGPHE, Skalskii N.	1960	GAK-3M GAK-4M	1:50,000 0.5x0.5	+/- 0.17
6	DGPHE, Stefankovich Z.	1961	GAK-3M	1:50,000 0.5x0.25	+/- 0.10
8	DGPHE, Antonov V.	1967	GAK-PT	1:200,000 5x2	+/- 0.32
9	DGRE, Kogal S.	1973-1974	GAK-PY GR/K-2	1:50,000 150.5	+/- 0.16
10	DGRE, Shuvatov Y.	1981-1984	GR/K-2	1:50,000 0.5x0.5	+/- 0.12
11	DGRE, Scharipov A.	1987-1990	GNU-KV GNU-KS	1:50,000 0.5x0.5	+/- 0.09

DGPHE - ZHEZKAZGAN Geophysical Exploration Expedition  
 DGRE - ZHEZKAZGAN Geological Exploration Expedition

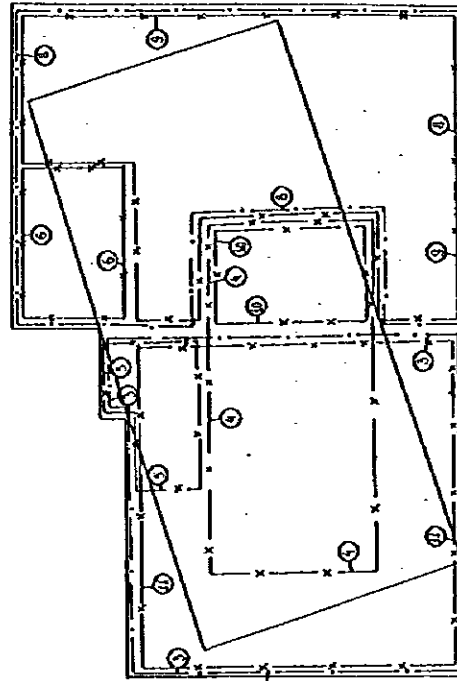


Table 2-1-5 Previous Electrical Surveys in the Zhaman-Albat Area

Index No.	Organization	Year	Equipment	Scale Network (km)	Accuracy (X)
1	AGPHE	1954	EP-1	1:100,000 SP Moving Schum 0.1x0.02	3-5
1.a	Stroitelova A			YES, IP	
2	DGPHE	1959	EP-1	1:100,000	max 5
	Skalaki N.			VES 2x1, 1x1, AB=1-4	
3	DGPHE	1960	EP-1	1:200,000	max 5
	Skalaki N.			VES 4x3, 2x1, AB= max 12	
4	DGPHE	1961	ESK-1	1:200,000	max 4, 6
	Stefankevich Z.			VES 4x3	
5	DGPHE	1967	ESK-1	1:200,000	max 5
	Antonov V.			VES, space=2, AB=1-1.5	
6	DGRE	1984	AE-72	1:50,000	3-2
	Schuvatov T.			VES, 1x1, 1x0.5, AB= max 1	
7	DGRE, Smirnova N	1986	VPS-63 CYCLE-2	Gradient IP, a=0.05, AB=1.6	< 5
				TEM, 1, 1, 0.1-2	
8	DGRE, Scharipov	1988	CYCLE-2	1:50,000	< 5
				TEM, space=0.5	

ZON - Western Geophysical Trust, AGPHE - Alatau Geophysical expedition

DGPHE - ZHEZKAZGAN Geophysical Exploration Expedition

DGRE - ZHEZKAZGAN Geological Exploration Expedition

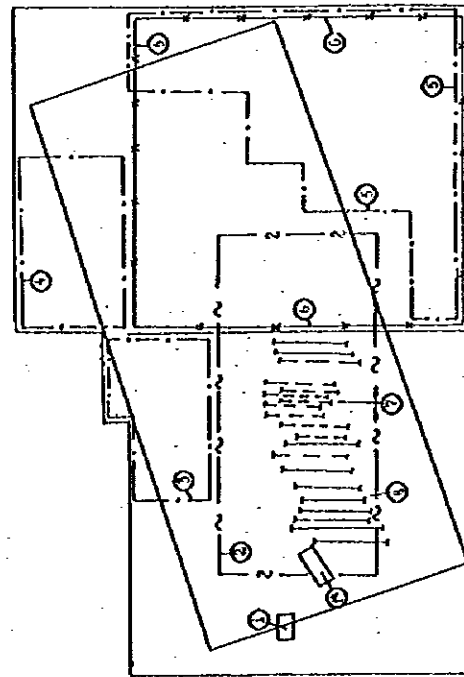
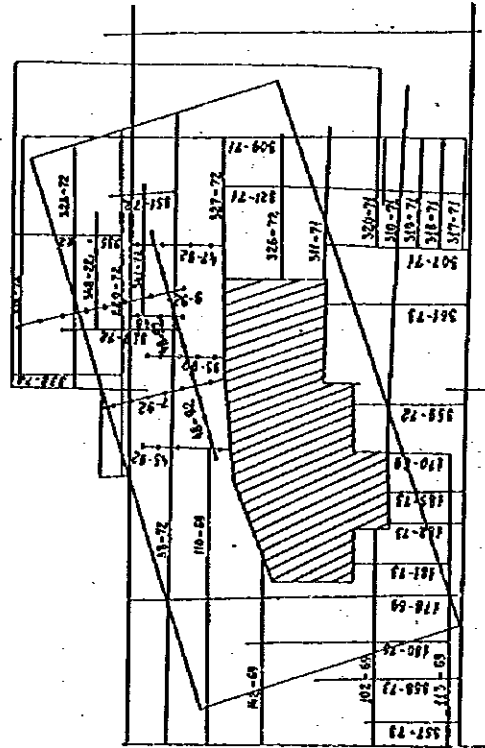


Table 2-1-6 Previous Seismic Surveys in the Zhaman-Albat Area

No.	Organization	Year	Instruments
1		1964-1974	MOV ( The reflection method )
2		1980-1992	MGG ( Common Depth Point )

DGPHE - ZHEZKAZGAN geophysical exploration expedition

DGRE - ZHEZKAZGAN geological exploration expedition



## 1-5 Ore Dressing Tests

The first ore dressing test using the ore samples from the Zhaman-Aibat Deposit was carried out (in accordance with the Zhezkazgantsuvtmet Flowsheet No.1 and No.2) by Parkhomenko L. P. in 1986. The test samples were composed of the Cu Ore (52kg, 2.12%Cu) and the Complex Ore (53kg, 2.21%Cu, 1.44%Pb, 1.83%Zn).

From 1990 to 1992, sixteen reports were prepared. In addition to the Cu Ore and the Complex Ore, subjects of the investigation were extended to a) Cu-Ag Ore, b) Pb-Zn Ore, c) Pb Ore, d) Zn Ore, e) Cu-Pb Ore, f) Cu-Zn Ore, g) Oxide Ore, h) Native Cu Ore. A summary of these reports is given in Appendix 1, and the representative reports are listed below.

- 1) Pask V.P., Chalova R.T., Krukova E.I. et. al. (1991): Report on testing in large scale laboratory conditions of dressing two ore samples from the Zhaman-Aibat Deposit, (Cu Ore:184kg, Cu-Pb Ore:268kg)
- 2) Malinova T.V. (1991): Study of dressing of 50 small scale technological samples of copper ores from the Zhaman-Aibat Deposit, for mapping aims, (Cu Ore:5 - 28kg)
- 3) Ivanova N.P. (1991): Study of dressing of sulfide copper-silver ores from the Zhaman-Aibat Deposit, (Cu-Ag Ore: 120 - 349kg)
- 4) Raykh M.A. (1991): Study of dressing of sulfide lead ores from the Zhaman-Aibat Deposit, (Pb Ore: 270kg)
- 5) Shamaeva T.S. (1991): Study of ore-dressing of 30 small scale technological samples of zinc, lead-zinc, copper-lead, copper-lead-zinc and copper-zinc ores from the Zhaman-Aibat Deposit (Zn Ore, Pb-Zn Ore, Cu-Pb Ore, Cu-Pb-Zn Ore, Cu-Zn Ore:5 - 16kg)
- 6) Malinova T.V. (1991): Study of ore-dressing of balance oxidized and sulfide copper ores from the Taskura Deposit (Cu Ore with oxide:180 - 208kg)
- 7) Malinova T.V. (1991): Study of dressing of sulfide zinc ores from the Zhaman-Aibat Deposit (Zn Ore:250kg)
- 8) Malinova T.V. (1992): Study of dressing of 12 small scale technological samples of copper ores from the Zhaman-Aibat Deposit, for mapping aims, (Cu Ore:5 - 22kg)
- 9) Shamaeva T.S. (1992): Results of ore dressing of sulfide lead ore in small scale technological sample No.121, (Pb Ore:8kg)
- 10) Malinova T.V. (1992): Study of dressing of small scale samples of sulfide ore with native copper from the Zhaman-Aibat Deposit (Cu Ore with native copper:15 - 53kg)

## Chapter 2 Geology and Ore Deposits

The geologic formations of the area range mainly from the Carboniferous to the Cretaceous in age. The absence of igneous and intrusive activities and significant thickness of sediments are characteristics of the geology in the area. The tectonic structure of the ore deposit area is related to the axial zone of the Zhaman-Aibat horst anticline, stretching in sub-latitudinal direction with steep northern and gentle southern limbs. The stratiform copper mineralization occurs exclusively in the grey-colored alluvial-deltaic sandstone facies within "Red Sandstone Formation" of the Carboniferous.

The geological map, stratigraphic column, schematic section, block diagram and isodepth map of ore horizon are shown in Fig.2-2-1, 2, 3, 4, 5.

### 2-1 Geology

#### 2-1-1 Stratigraphy

##### a) Paleozoic group (Pz)

##### a)-1 Carboniferous system (C)

Carboniferous system in the Zhaman-Aibat Area is divided into the Serpukhov Formation, Taskuduk Formation and Zhezkazgan Formation in ascending order. The Serpukhov Formation is correlative with the Lower Carboniferous, the Taskuduk Formation and Zhezkazgan Formation are correlative with the Middle to Upper Carboniferous. Carbonaceous terrigenous complex of marine sediment is included in the lower series and a complex of various accumulations of continental origin in the middle to upper series.

##### Serpukhov Stage (C<sub>1s</sub>)

Fine grained limestone, red sandstone and red aleurolite, aleurolite with interlayers of grey sandstone. The number of terrigenous rocks decreases at lower levels where there are interlayers of limestone in horizons of calcareous aleurolite. Total thickness is approximately 750m.

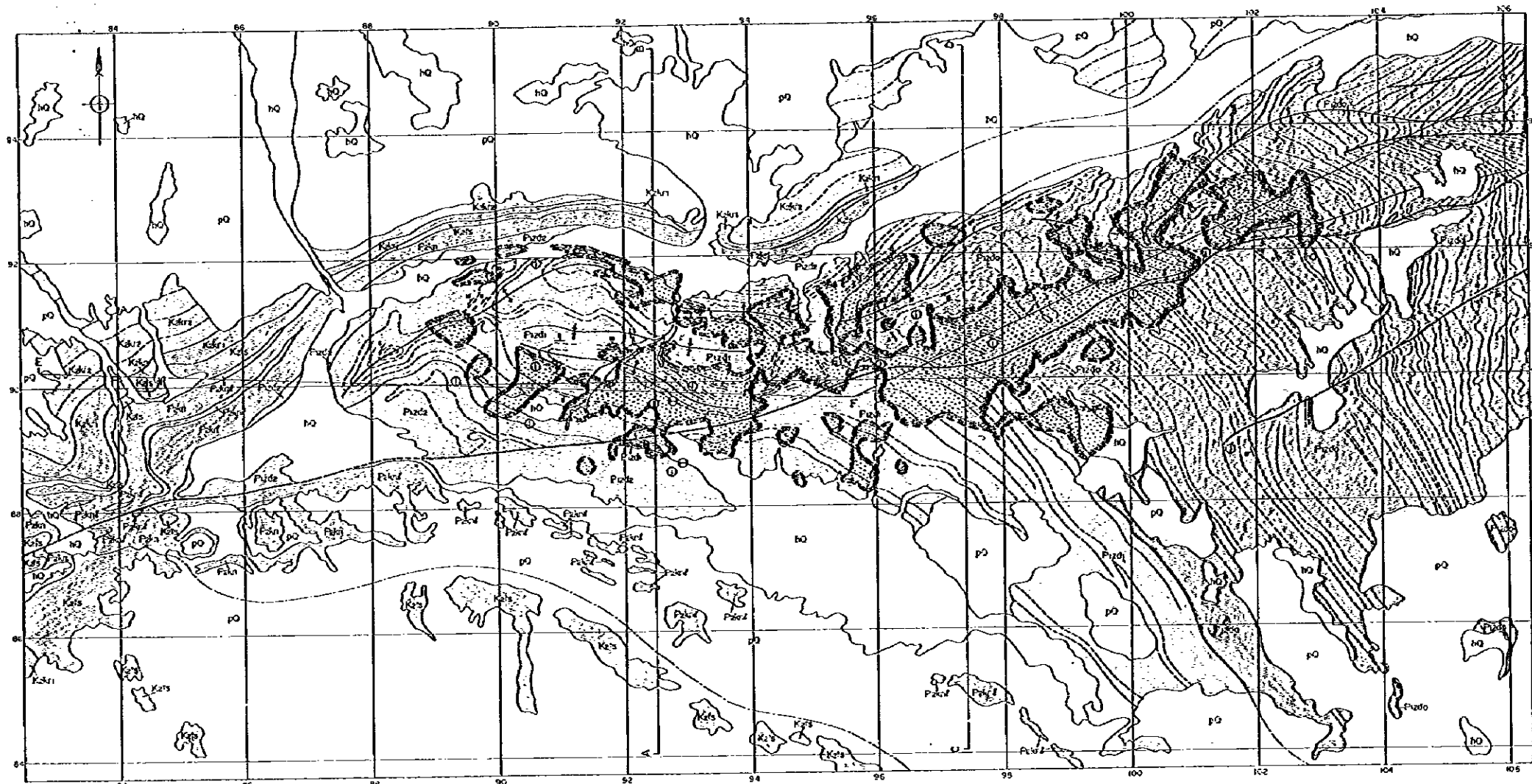
##### Taskuduk Formation (C<sub>2ts</sub>)

Sediments of the Taskuduk Formation are deposited conformably on sediments of the Serpukhov Formation and are overlaid (with washout) by the sediments of the Zhezkazgan Formation. They are outcropping at the anticlinal structure in the eastern part of the area. The upper boundary with the Zhezkazgan Formation follows the horizon of interformational conglomerate (Raimundo conglomerate) at the bottom boundary, and has a roof of limestone with fauna.

Sediments of the Taskuduk Formation are represented by interbedded terrigenous rocks,







**LEGEND**

- Geological Series**
  - Kz** Kizilsay Formation
  - Pz** Paleozoic
- Geological Systems**
  - Kz1** Karakul Formation
  - Kz2** Karakul Formation
  - Kz3** Karakul Formation
  - Kz4** Karakul Formation
  - Kz5** Karakul Formation
  - Kz6** Karakul Formation
  - Kz7** Karakul Formation
  - Kz8** Karakul Formation
  - Kz9** Karakul Formation
  - Kz10** Karakul Formation
  - Kz11** Karakul Formation
  - Kz12** Karakul Formation
  - Kz13** Karakul Formation
  - Kz14** Karakul Formation
  - Kz15** Karakul Formation
  - Kz16** Karakul Formation
  - Kz17** Karakul Formation
  - Kz18** Karakul Formation
  - Kz19** Karakul Formation
  - Kz20** Karakul Formation
  - Kz21** Karakul Formation
  - Kz22** Karakul Formation
  - Kz23** Karakul Formation
  - Kz24** Karakul Formation
  - Kz25** Karakul Formation
  - Kz26** Karakul Formation
  - Kz27** Karakul Formation
  - Kz28** Karakul Formation
  - Kz29** Karakul Formation
  - Kz30** Karakul Formation
  - Kz31** Karakul Formation
  - Kz32** Karakul Formation
  - Kz33** Karakul Formation
  - Kz34** Karakul Formation
  - Kz35** Karakul Formation
  - Kz36** Karakul Formation
  - Kz37** Karakul Formation
  - Kz38** Karakul Formation
  - Kz39** Karakul Formation
  - Kz40** Karakul Formation
  - Kz41** Karakul Formation
  - Kz42** Karakul Formation
  - Kz43** Karakul Formation
  - Kz44** Karakul Formation
  - Kz45** Karakul Formation
  - Kz46** Karakul Formation
  - Kz47** Karakul Formation
  - Kz48** Karakul Formation
  - Kz49** Karakul Formation
  - Kz50** Karakul Formation
  - Kz51** Karakul Formation
  - Kz52** Karakul Formation
  - Kz53** Karakul Formation
  - Kz54** Karakul Formation
  - Kz55** Karakul Formation
  - Kz56** Karakul Formation
  - Kz57** Karakul Formation
  - Kz58** Karakul Formation
  - Kz59** Karakul Formation
  - Kz60** Karakul Formation
  - Kz61** Karakul Formation
  - Kz62** Karakul Formation
  - Kz63** Karakul Formation
  - Kz64** Karakul Formation
  - Kz65** Karakul Formation
  - Kz66** Karakul Formation
  - Kz67** Karakul Formation
  - Kz68** Karakul Formation
  - Kz69** Karakul Formation
  - Kz70** Karakul Formation
  - Kz71** Karakul Formation
  - Kz72** Karakul Formation
  - Kz73** Karakul Formation
  - Kz74** Karakul Formation
  - Kz75** Karakul Formation
  - Kz76** Karakul Formation
  - Kz77** Karakul Formation
  - Kz78** Karakul Formation
  - Kz79** Karakul Formation
  - Kz80** Karakul Formation
  - Kz81** Karakul Formation
  - Kz82** Karakul Formation
  - Kz83** Karakul Formation
  - Kz84** Karakul Formation
  - Kz85** Karakul Formation
  - Kz86** Karakul Formation
  - Kz87** Karakul Formation
  - Kz88** Karakul Formation
  - Kz89** Karakul Formation
  - Kz90** Karakul Formation
  - Kz91** Karakul Formation
  - Kz92** Karakul Formation
  - Kz93** Karakul Formation
  - Kz94** Karakul Formation
  - Kz95** Karakul Formation
  - Kz96** Karakul Formation
  - Kz97** Karakul Formation
  - Kz98** Karakul Formation
  - Kz99** Karakul Formation
  - Kz100** Karakul Formation

- Geological boundary
- Geological boundary, covered by alluvial deposits
- Bedding structure
- Fault
- Fault, covered by alluvial deposits
- Basin axis
- Structure
- Basin, by accident (D-3)
- Outline of the body (D-3, D-4, D-5)
- Line of section
- Geological column
- Structural structure

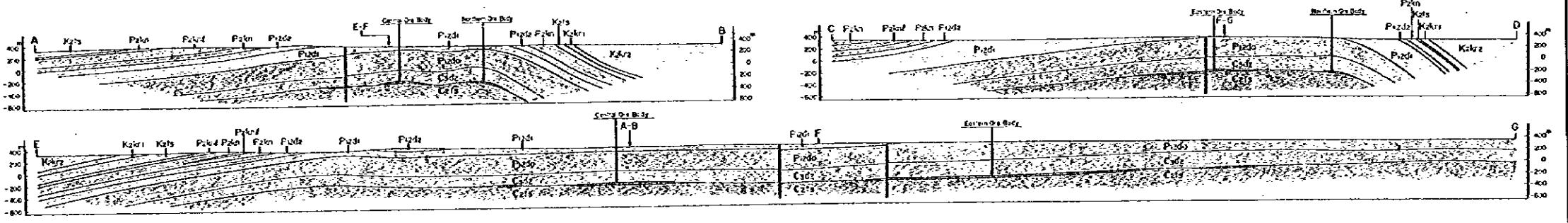


**Fig.2-2-1 Geological Map of the Zhaman-Albat Area**



Geologic Age		Formation		Columnar Section	Thickness (m)	Mineralization	Ore Formation	Cuprous Stratum	Ore Deposit	
Cenozoic	Quaternary		Q <sub>v</sub>		2	↕	Rhodsite-gypsum-salt "Evaporite type"	Mansfeld type	Taskura	
			Q <sub>4v</sub>		3					
			Q <sub>3n</sub>		15					
	Paleogene	Set-pag-dalyn		Q <sub>0-ψ</sub>						2~3
				P3bf						1~40
				P2Cq						16
Mesozoic	Cretaceous	Karakoin								
				K2kr						100
		Tacura		K2ls						100-
Paleozoic	Permian	Upper	Kengir	P1-zkn						100+
		Lower	Zhidelsal		P1zd					
	Carboniferous	Upper	Zhezkazgan		C2-3dz		150 300			
		Middle	Taskuduk		C2lz		60 600			
Lower	Serpukhov		C1s		750					

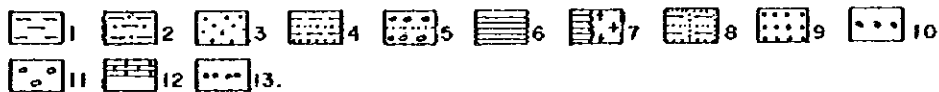


Fig.2-2-2 Stratigraphic Column of the Zhaman-Albat Area

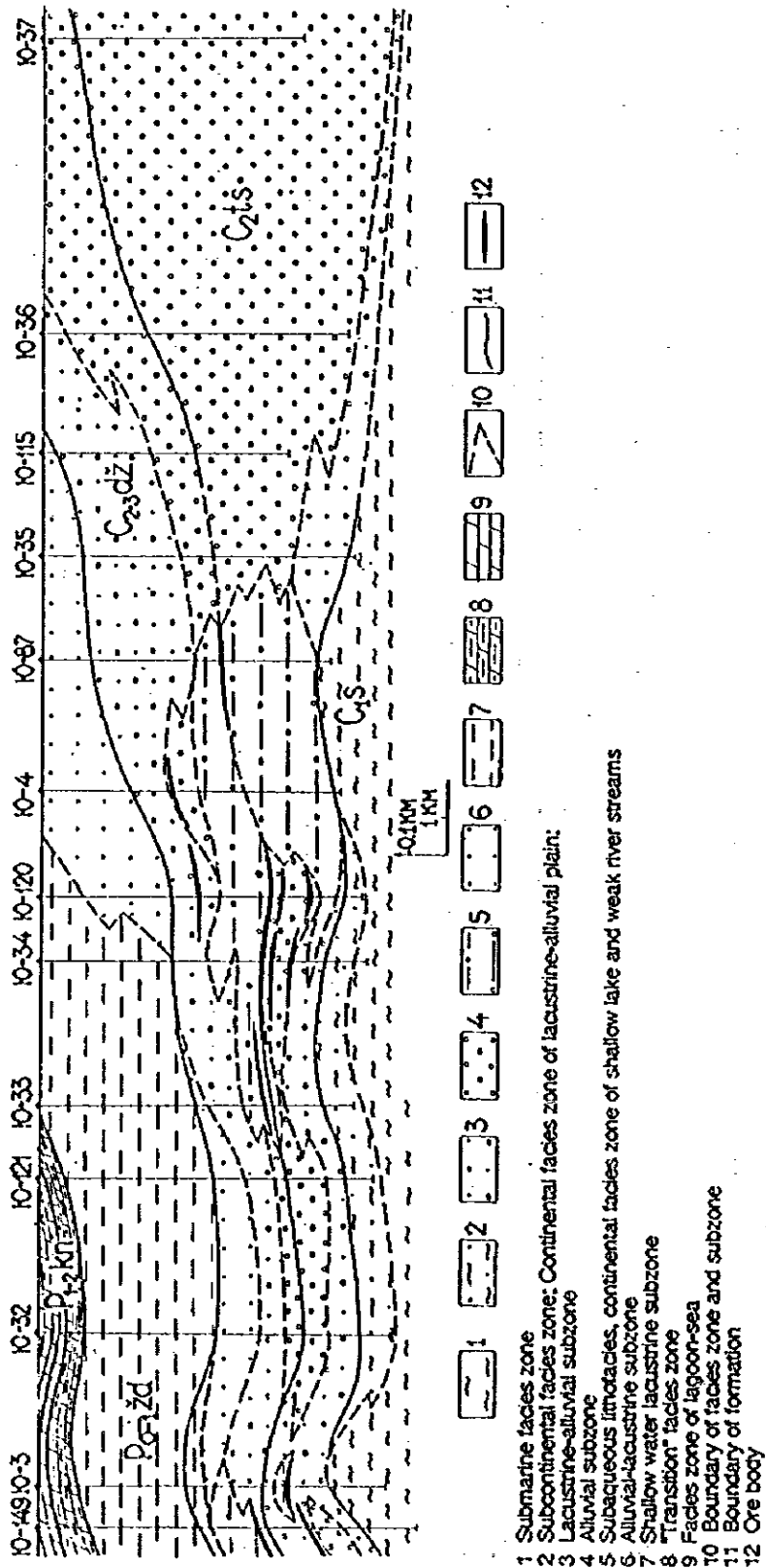


Fig. 2-2-3 Schematic Section of the Zhaman-Albat Area

(from Glybovski V.O., 1988)



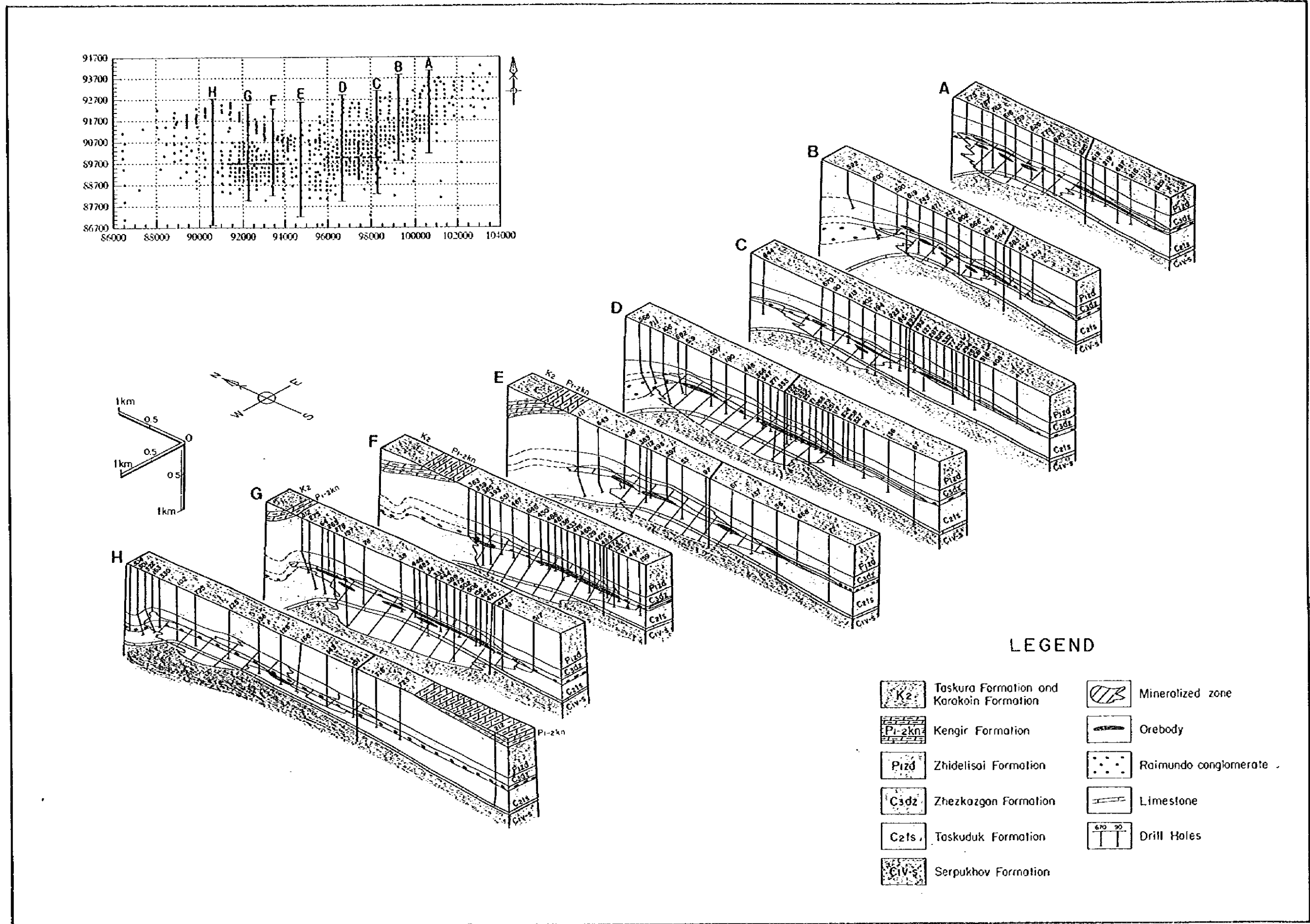


Fig. 2-2-4 Block Diagram of the Zhaman-Aibat Area



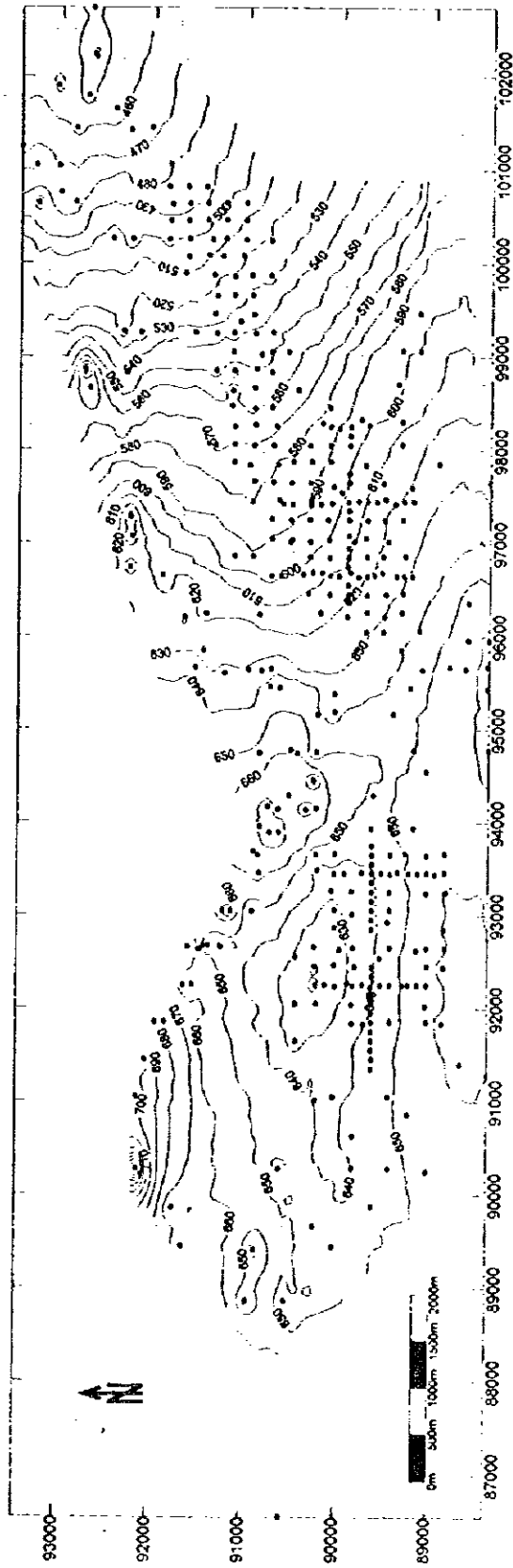


Fig.2-2-5 Depth to the Base of Zhezkazgan Formation in the Zhaman-Albat Area



formed under the conditions of coastal and alluvial plain. They are constituted by reddish and greyish fine-grained sandstone and aleurolite. Interlayers of conglomerate with partly rounded gravels of red rock and carbonate rocks are included. Sediments of the formation have not been age-determined paleontologically. The thickness of the formation varies from 60 - 70m at the axial part of the western part of the horst anticline, to 600m or more at the eastern, northern and southern wings.

#### **Zhezkazgan Formation (C2-3d2)**

The rocks of the Zhezkazgan Formation are well distributed in the eastern flank of the depression at the core of the anticlinal structure, 5 km from the survey area. Sediments of the Zhezkazgan Formation are deposited unconformably on the Taskuduk Formation with the interformational conglomerate (Raimundo conglomerate) at the bottom, and are conformably overlaid by the sediments of the Zhidelisai Formation. The upper boundary with the Zhidelisai Formation is conventionally delineated along the roof of grey fine-grained sandstone.

Sediments of the Formation are represented by red laminated sandstone, aleurolite and grey sandstone, rarely aleurolite with interformational conglomerate with interlayers of sedimentary breccia and interformational conglomerate (Raimundo), mentioned above. Sediments of both the Zhezkazgan and the Taskuduk Formation are represented by rhythmical interbedding of terrigenous rocks formed under the condition of alluvial plain.

The thickness of the Formation in the deposit area is 180 - 200m, and on the flanks it is estimated to be 300m and more. The increase of the thickness of grey sandstone at the bottom of the Formation is typical of cross sections of the Zhaman-Aibat Deposit, in which commercial grades of copper, lead and zinc were detected as a result of prospecting (Fig. 2-2-4).

#### **a)-2 Permian system (P)**

Sediments of the Zhidelisai Formation with terrigenous composition are defined within the Lower Permian system, and the Sediments of the Kengir Formations with carbonate composition, respectively, are correlative with the Lower to Middle Permian system.

#### **Zhidelisai Formation (P12d)**

The sediments of the Zhidelisai Formation are widely distributed in the area and form the core and wings of the anticlinal structure on the surface, and are penetrated by a number of prospecting drillholes. The Formation is conformably covered by the Kengir Formation.

The sediments of the Formation are everywhere represented by obliquely laminated red aleurolite and sandstone with interlayers of brown (grey-red) fine grained sandstone. The presence of gypsum and anhydrite is typical for the entire cross section and rock salt at the flanks of the structure, i. e., at the southern and western parts. The presence of rock salt, anhydrite and gypsum among red rocks of the Zhidelisai Formation make it possible to include in the evaporite complex of rocks formed under the conditions of hot climate at flood plain and lake faces.

The thickness of sediments on the western flank is approximately 300m. On the northern

flank it is estimated to be 540m and more.

#### **Kengir Formation (P1-2kn)**

Sediments of the Kengir Formation are out-cropping only in the western part of the anticlinal structure and are penetrated by a number of drillholes. They are deposited conformably on the Zhidelisai Formation and are unconformably overlaid by the Mesozoic-Cenozoic sediments.

The Formation is represented by grey and dark grey marls, oolitic horizontal-layered limestone, limy aleurolite and sandstone. Large amounts of gypsum in the lower part of the cross section of the Formation is typical. The copper deposit in the Taskura is represented both by oxidized and sulphide ores and occurs locally in the sediment of the Kengir Formation.

The thickness of sediments on the western flank is approximately 300m and more.

### **b) Mesozoic Group (Mz)**

#### **Cretaceous system (K)**

##### **Taskura Formation (K2ts)**

Sediments of the Upper Cretaceous are deposited at sharp unconformity angles on the washed out surfaces of more ancient formations and are overlapped by the Cenozoic sediment of various ages. They are represented by alternations of grey and green opoka-like aleurolite, clays, inequigranular sandstone, conglomerate and marl. The thickness of sediment does not exceed 100m.

##### **Karakoin Formation (K2kr)**

Sediments of the Karakoin Formation are deposited unconformably on those of the Taskura Formation and are unconformably overlain by the Cenozoic sediment. Pebble to granule size conglomerates are observed at the bottom and alternations of eolian and speckled clay correspond to the middle and the upper.

### **c) Cenozoic Group (Kz)**

#### **c)-1 Paleogene system (P)**

The Paleocene-Eocene sediments (P1-2) overlie the Paleozoic and the Mesozoic formations of different ages and are represented by lenticular interbedded clay of various colors, aleurolite, sandstone with separate lenses of quartz-like sandstone. The thickness of sediment is 20 - 30m and reaches 120m in depressions. Sediments of the Betpakdalin Formation of the Oligon age are widely distributed in the survey area and are represented by red, red-brown, brown and green clay with gypsum and manganese oxide with interlayers of aleurolite of brown color and clayey sand. The thickness of the sediment is 1 - 40m.

## c)-2 Quaternary system (Q)

Quaternary system is represented by formation of various genetic types. Total thickness does not exceed 10m. The composition;

- ① Middle-Upper-Quaternary eolian sand and aleurolite with admixtures of gravel;
- ② Upper-Quaternary-Contemporary proluvium-deluvium loam, clayey sand, gravel;
- ③ Contemporary "Takyr"-salsifies clay, aleuroite.

## 2-1-2 Tectonic Structure

The survey area is located at the zone of intersection of the Chu-Ili anticlinorium with the eastern edge of the Zhezkazgan Sarysu depression. The Chu-Ili anticlinorium is represented by a linearly-stretched, folded structure, subsiding to the southwest under the cover of the sedimentary rocks, which form the Zhezkazgan - Sarysu depression, the border between these two structures follows the Bekei deep-seated fault. From consideration of the character of the folding structure and lithology of the formations, four stages are defined:

(1) **Early Paleozoic geosynclinal stage:** This structural stage is represented by sediment of Vendian-Cambrian and the middle to upper Ordovician, which are folded into narrow linear folds in the northwestern direction. Folds are compiled by ruptured dislocation of faults. Sediments of this stage with sharp unconformity are overlain by orogenic formations.

(2) **Devonian orogenic stage:** This orogenic stage includes the volcanic rock mass of the lower to middle Devonian. The rock mass is composed of rather large and is overlain by anticlinal structures.

(3) **Carboniferous - Permian subplatform stage:** This orogenic stage is formed by terrigenous carbonate rocks of the upper Paleozoic. These sediments are most widely spread and they participate in the formation of the Zhezkazgan-Sarysu depression. Sub-lateral anticlinal structures are developed on the eastern flank of the Taskura-Tasbulak trough, which have the shape of a nose structure similar to the Zhaman-Aibat anticline. The absence of intrusive activity and significant thickness of sediments are typical for this structural stage.

(4) **Mesozoic-Cenozoic stage:** This structure is formed by gently pitching, mainly ferrigenous rocks of marine and continental origin, classified as Jurassic, Cretaceous, Paleogene and Quaternary period with a Mesozoic crust of erosion at the bottom. Sediments of Mesozoic-Cenozoic are referred to typically as platform sediments. The structure of the area is determined by faults of northwestern and sub-longitudinal strike. The former faults are of the most ancient Caledonian stage and the Bekei deep-seated fault, separating the Chu-Ili anticlinorium from the Zhezkazgan-Sarysu depression, is a typical representative of this type. The latter faults represent the other type of dislocations in younger age and cut faults of the former direction and control the orientation of local folded structures. They are classified as overlap fault and have steep dislocations.

## **2-2 Ore Deposits**

### **2-2-1 Ore Stratigraphy**

Copper mineralization in the Zhaman-Aibat Deposit occurs in interlayers of grey-colored sandstone, gravelstone and conglomerates, rarely aleuro-sandstone and aleuro-argillite. Commercial grade mineralization is concentrated mainly in the coarse-grained fractions which as a rule have secondary (epigenetic) grey color and are composed of lower element-faces of cyclothem (rhythms) of alluvial character. Fine grained primary (syngenetic) grey subaqueous lithofaces contain little or no ore (Fig.2-2-6).

It is possible to consider that the lithological composition of the Permian-Carboniferous red sediment and petrography of the Zhaman-Aibat Area do not greatly differ from that of the Zhezkazgan Area formations. As in the Zhezkazgan ore field, the cross section of productive sediments within the ore field of the Zhaman-Aibat Deposit has been preliminarily divided into ore-bearing horizons. The availability of reliable markers (key beds), such as organogenic limestone of the Serpukhov stage, interformational conglomerate and gravel of Raimundo type and relative persistence of interlayers of grey sandstone make such division appropriate (Fig.2-2-14, Fig.2-2-15).

In compliance with this, it is considered that the Taskuduk Formation contains five horizons, the Zhezkazgan Formation six horizons and the Zhidelisai Formation one horizon. Major commercial mineralization is confined to the Horizon 4-I which occurs some 1 - 4m above the interformational (Raimundo) conglomerate (Plates 9 and 10). Zhezkazgangeologiya estimated that approximately 90% of the copper ore is concentrated within Horizon 4-I. Another major mineralization is defined as Horizon 3-VI; stratigraphically this horizon is located 20-30m below than Horizon 4-I.

### **2-2-2 Occurrence of Ore**

There are three main orebodies, namely the Central, Northern and Eastern Orebodies (Table 2-2-3). These orebodies are distributed in an area with dimensions: approximately 12.5km in the east-west direction and approximately 5km in the north-south direction. The depth of Horizon 4-I is approximately 460 - 480m in the eastern area and the depth increases toward the west. At the western edge of the Central Orebody it reaches 650m. At the north western edge of the Northern Orebody, the maximum depth was confirmed to be 710m (Fig.2-2-5, 2-2-16, 2-2-17). The morphology of each orebody shows a mant-like, lens-shape or band like shape with complex inner mineral structures.

### **2-2-3 Mineral Assemblage and Ore Texture**

Studies of mineral composition of ores at the Zhaman-Aibat Deposit started in 1983 and 1,450 polished thin sections have been scanned mainly by the Kazakhstan Science-Research Institute (Table 2-2-1). More than 30 minerals, falling within groups of native elements, sulfides, arsenides, oxides and sulphates, have been reported. The mineral composition of the ore is comparatively

simple. The main minerals are chalcocite group minerals, such as chalcocite with digenite and djurleite, bornite, galena and chalcopyrite in small amounts. Accessory minerals are pyrite, marcasite, sphalerite, tennantite as primary minerals and covellite, native silver and native copper as secondary minerals.

The following micro structures are typical for ore minerals in the deposit: evenly impregnated, impregnated spotted, banded, interstitial, cemented inherited and rarely veinlet. In the high grade copper ore, copper minerals, mainly chalcocite are completely impregnated and represent a massive ore. Normal grade copper ore contains chalcocite and minor amounts of bornite impregnated in the matrix among grains of sandstone or siltstone (aleurolite). The ore fabric is often banded being defined by the sedimentary structure of sandstone.

Ore zonation in the Zhaman-Aibat Deposit has been discussed in the previous geological and mineralogical study reports (Fig.2-2-18). The development of more robust models of zonation await further evaluation of previous data, which will provide useful information on ore genesis of the Zhaman-Aibat copper deposit.

#### 2-2-4 Ore Type

With the assemblage of ore minerals, several ore types, namely Copper Ore, Complex Ore, Lead-Zinc Ore and Silver Ore are classified by the Zhezkazgangeologiya (Table 2-2-2). Major ore types are confined to the Copper Ore and Complex Ore. Based on the result of ore reserve (geological resources) estimation by the Japanese survey team, the Copper Ore and Complex Ore account for 98% of total ore reserves (Table 2-3-6).

Copper Ore shows simple mineral assemblage, it is composed of chalcocite group minerals (mainly chalcocite, with small amounts of djurleite and digenite) and bornite. Copper Ore occurs widely in the Zhaman-Aibat Deposit, frequently representing the richest zones of ore deposits. It is characterized by impregnated striped, spotted and inherited cement structure. Silver is associated with chalcocite ores as silver rich electrum, stromeyerite and native Ag (not confirmed yet in this year's campaign). This type of ore is predominant in the Eastern Orebody.

The complex ore shows several types of the mineral assemblage. Chalcocite-bornite-galena type widely spread mainly in the Central Orebody and partially in the Northern Orebody. In the Central Orebody it represents the most rich, even massive complex ores. Chalcopyrite-galena type ore is widely spread and is relatively poor complex ore of Taskuduk and Zhezkazgan Formation. Chalcocite-bornite-galena-sphalerite type is rare and occurs sporadically in sediments of the Zhezkazgan Formation in the Central Orebody and rarely in the Eastern Orebody. Chalcopyrite-galena-sphalerite type is moderately well distributed in the area. Chalcocite-sphalerite type is rather rare and represents an intensive impregnated structure.

Table 2-2-1 List of Minerals Described in the Previous Studies  
in the Zhama-Aibat Ore deposit (Botsmanovsky(1991))

Main		Accessory		Rare	
chalcocite	Cu <sub>2</sub> S	pyrite	FeS <sub>2</sub>	β-domeykite	Cu <sub>3</sub> As
digenite	Cu <sub>11</sub> 8S	marcasite	FeS <sub>2</sub>	algodonite	Cu <sub>6</sub> As
djurleite	Cu <sub>11</sub> 6S	covellite	CuS	stromeyerite	CuAgS
bornite	Cu <sub>5</sub> FeS <sub>4</sub>	sphalerite	ZnS	native copper	Cu
galena	PbS	tennantite	(Cu,Fe) <sub>12</sub> As <sub>4</sub> S <sub>13</sub>	arsenopyrite	FeAsS
chalcopyrite	CuFeS <sub>2</sub>	native silver	Ag	loellingite	FeAs <sub>2</sub> ·x
				koutekite*	Cu <sub>5</sub> As <sub>2</sub>
				kutinaite*	Cu <sub>2</sub> AgAs
				scutterudite**	CoAs <sub>3</sub>
				pyrrhotite**	Fe <sub>1-x</sub> S
				betekhtinite***	Cu <sub>2</sub> Pb <sub>2</sub> S <sub>15</sub>
				graphite	C
				lepidocrocite	FeOOH
				cuprite****	Cu <sub>2</sub> O
				anglesite****	PbSO <sub>4</sub>
				sufflorite***	(Co,Fe)As <sub>2</sub>
				cobaltite***	(Co,Fe)AsS

\*: minerals, firstly described in the USSR;

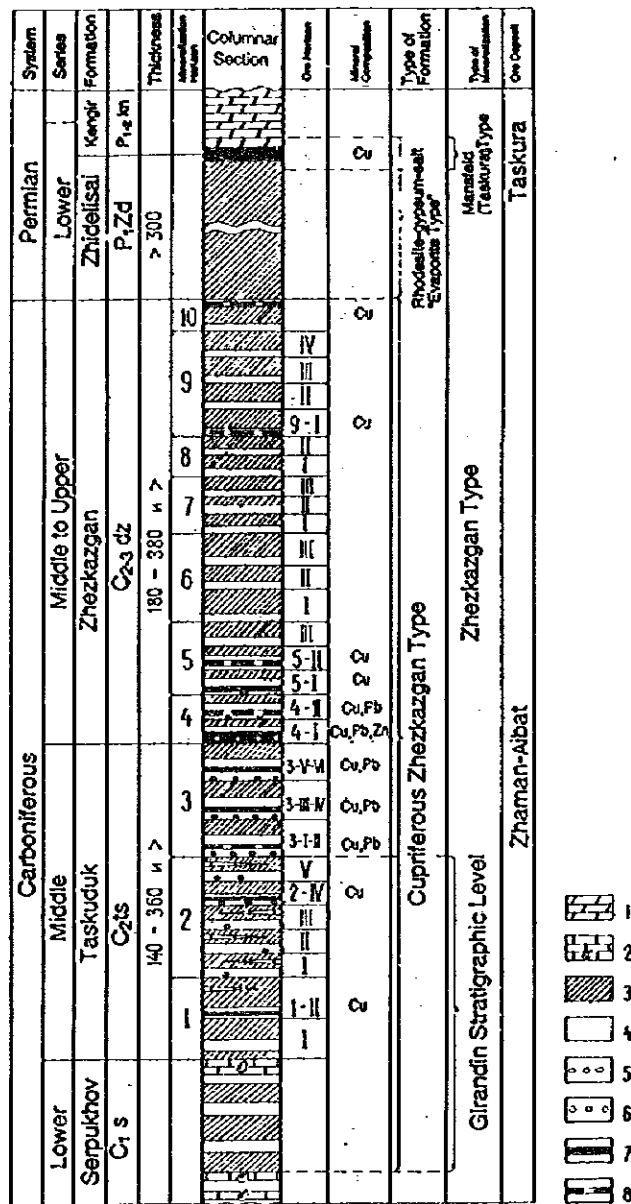
\*\* : minerals, firstly described at cupreous sandstone deposits at Zhezkazgan survey area;

\*\*\*: minerals, requiring additional methods of diagnostics;

\*\*\*\*: minerals of doubtful hypogenic origin.

Table 2-2-2 Ore Classification and Cut Off Grade by GezkazganGeologia

	Cu	Pb+Zn	Ag	Minimum Commercial Grade (Dec. 1991)
Copper Ore	0.40% ≤ Cu	Pb+Zn < 0.80%	-	0.75% ≤ Cu
Complex Ore	0.30% ≤ Cu	0.80% ≤ Pb+Zn	-	0.85% ≤ Pb+Zn
Lead-Zinc Ore	Cu < 0.30%	1.10% ≤ Pb+Zn	-	2.25% ≤ Pb+Zn
Silver Ore	Cu < 0.30%	Pb+Zn < 1.10%	5g/t ≤ Ag	14g/t ≤ Ag
	0.30% ≤ Cu < 0.40%	Pb+Zn < 0.80%	5g/t ≤ Ag	



Glybovskii V. O. (1989)

1 - Marl ; 2 - Limestone ; 3 - Red Aleuro-Argillite ; 4 - Grey Sandstone ; 5 - Intra Formation Conglomerate ; 6 - "Raimundo" Conglomerate and Gravelite ; 7 - Assumed Commercial Grade Mineralization ; 8 - Assumed Low Grade Mineralization.

Fig.2-2-6 Stratigraphic Column of Cupriferous Sediments in the Zhaman-Albat Area





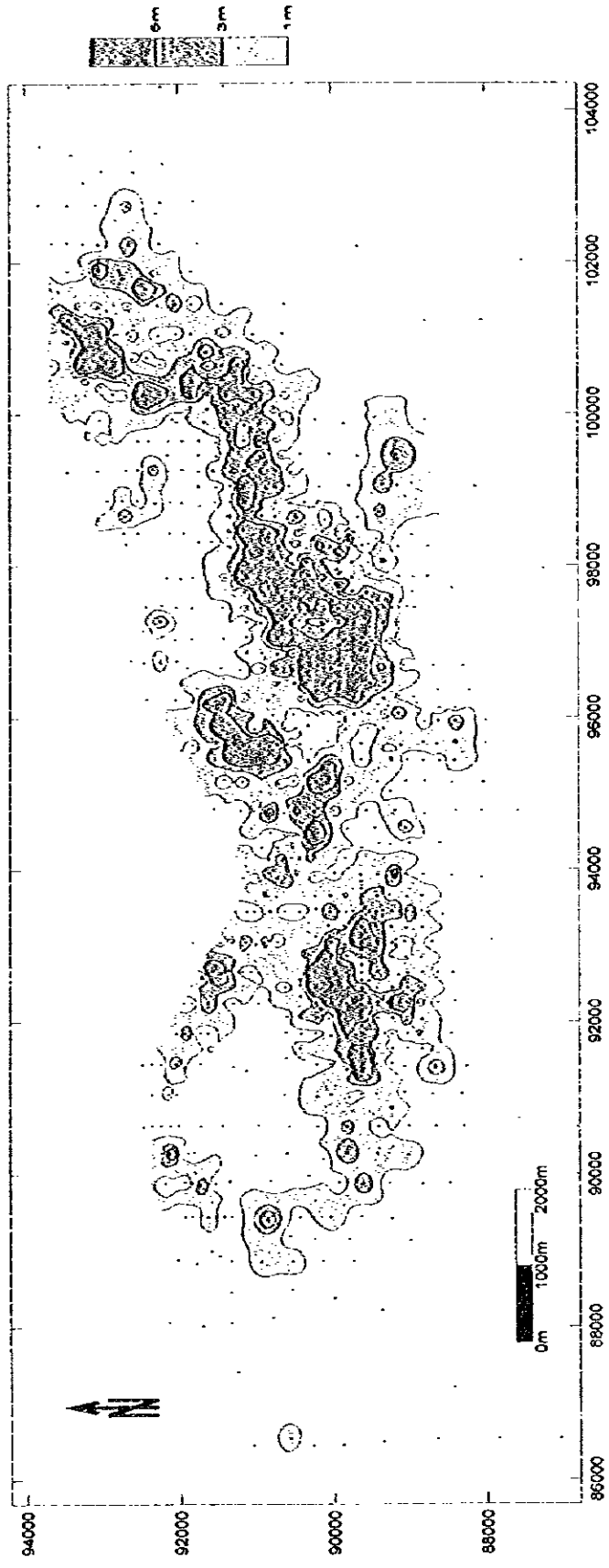


Fig.2-2-7 Thickness of the 4-l Ore Horizon in the Zhaman-Aibat Area

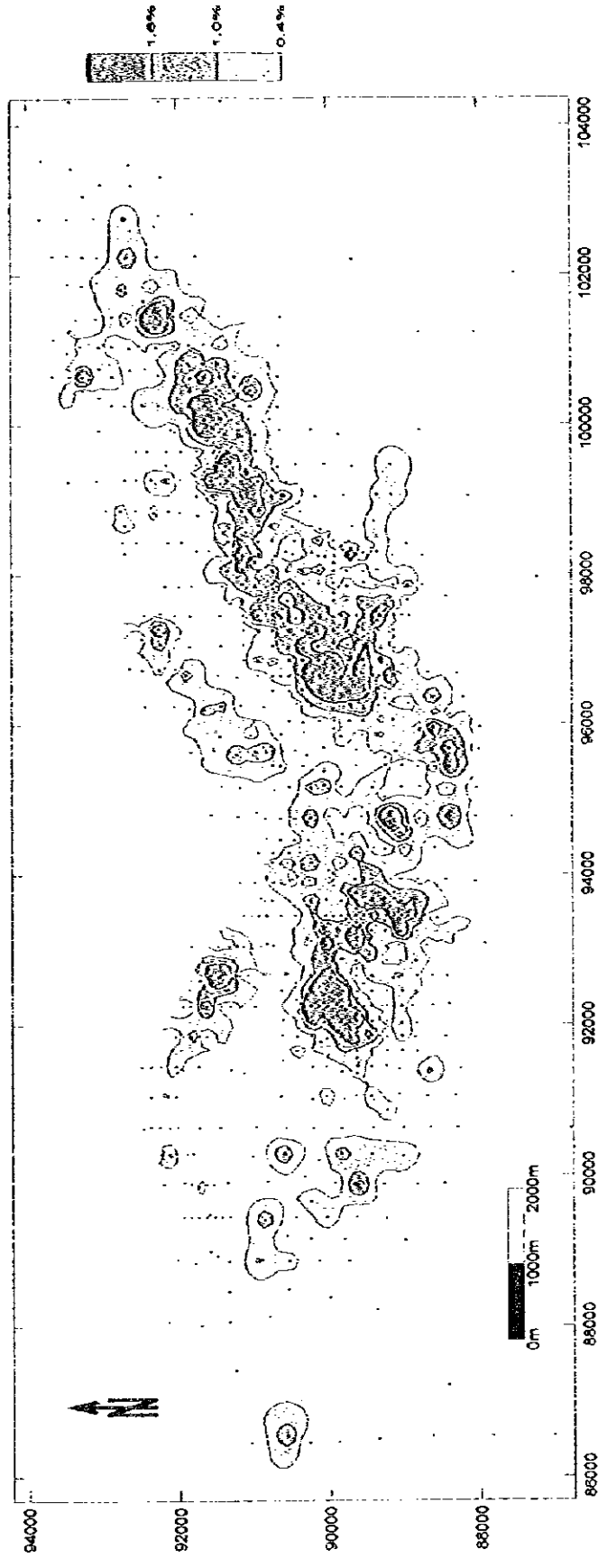


Fig.2-2-8 Cu Grade of the 4-l Ore Horizon in the Zhaman-Aibat Area

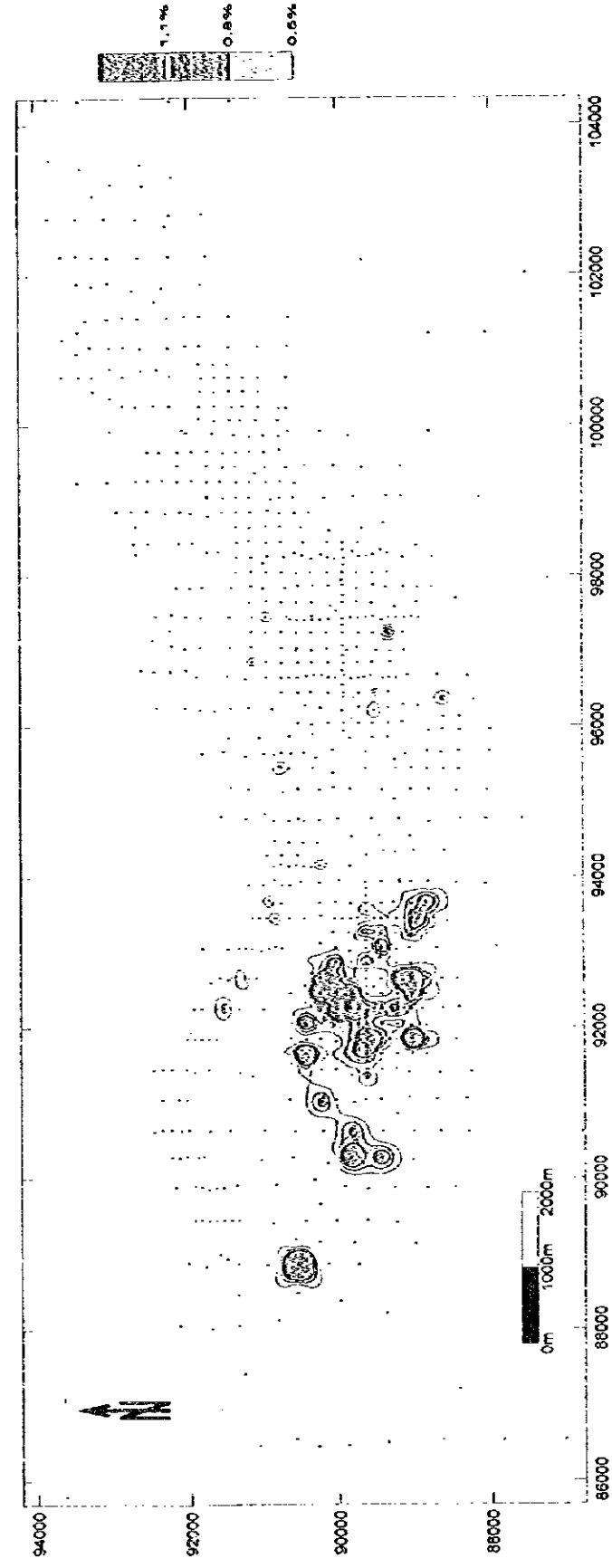


Fig.2-2-9 Pb Grade of the 4-l Ore Horizon in the Zhaman-Aibat Area

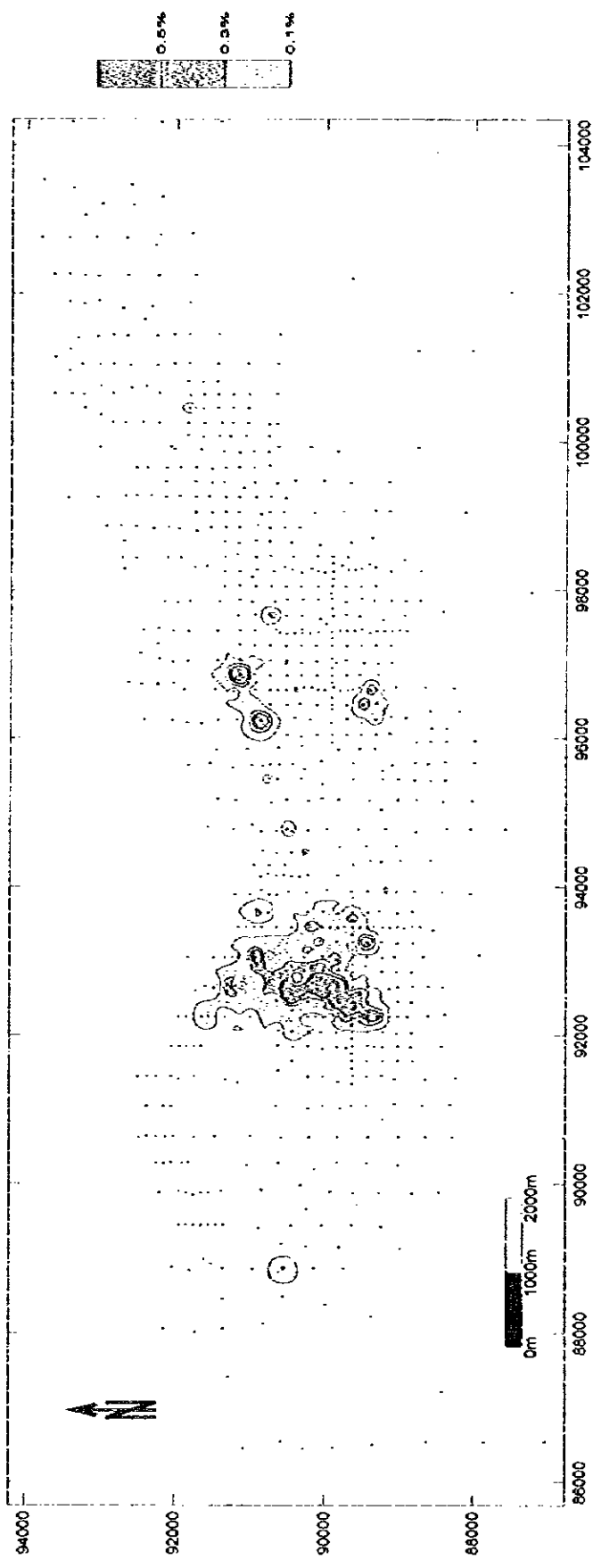


Fig.2-2-10 Zn Grade of the 4-l Ore Horizon in the Zhama-Aibat Area

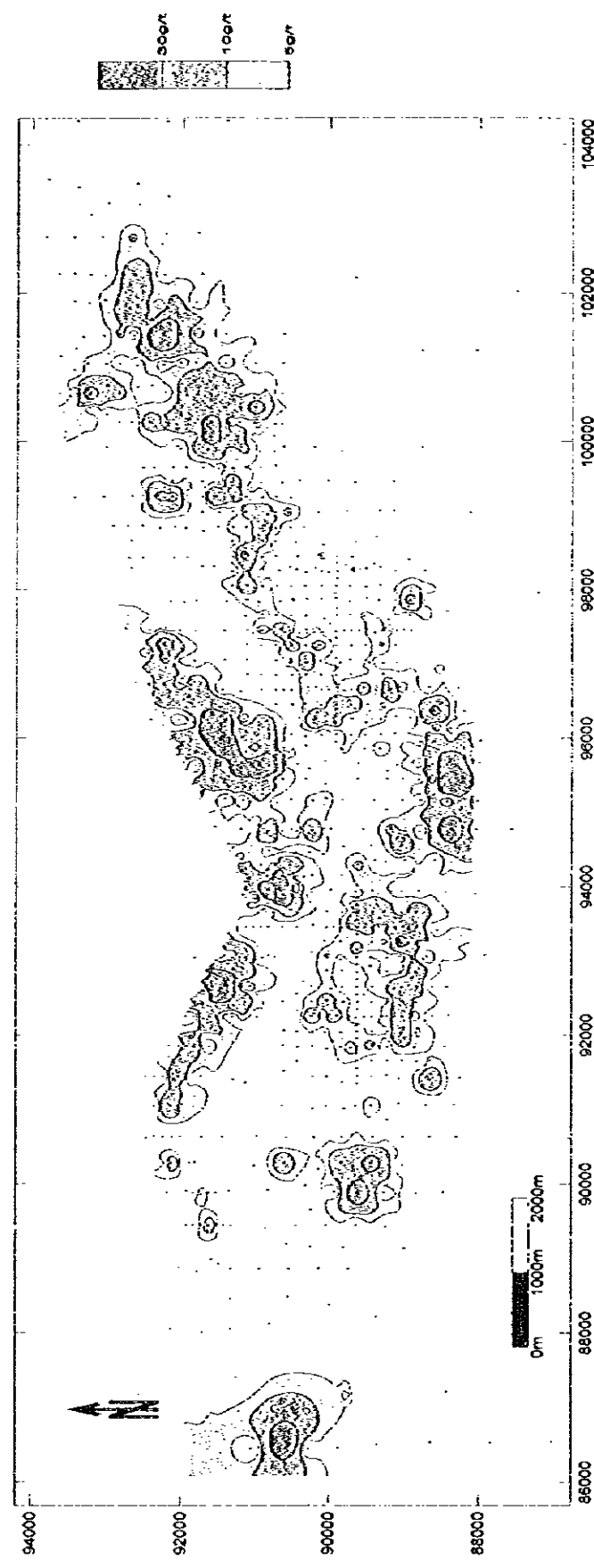


Fig.2-2-11 Ag Grade of the 4-l Ore Horizon in the Zhama-Aibat Area

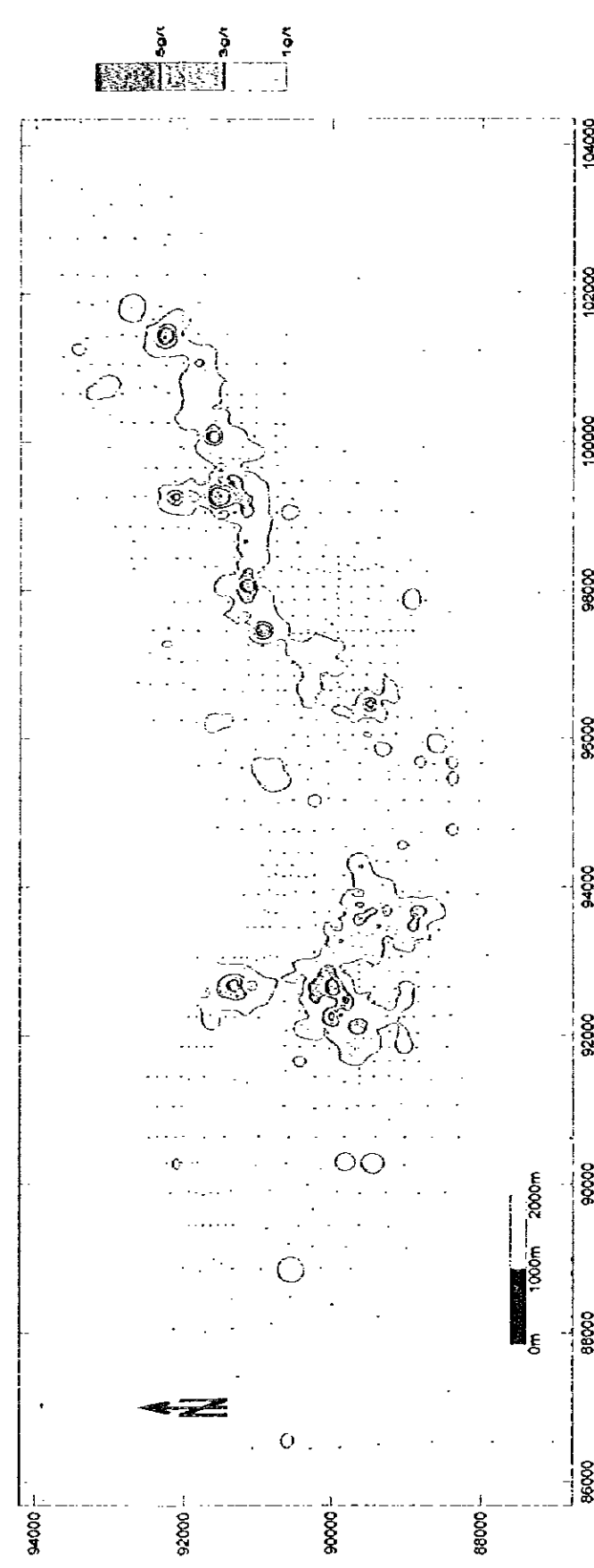
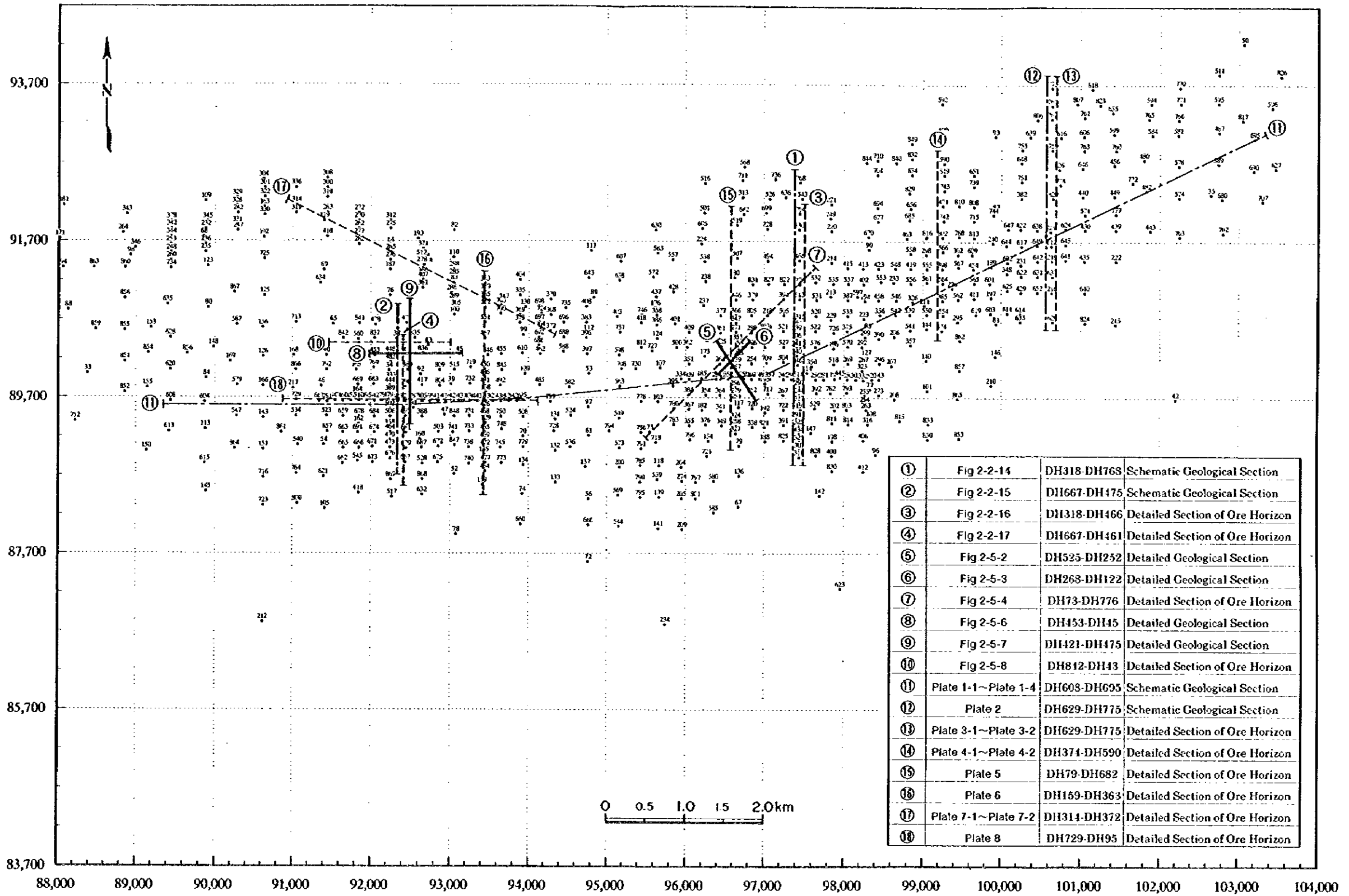


Fig.2-2-12 Re Grade of the 4-l Ore Horizon in the Zhama-Aibat Area



①	Fig 2-2-14	DH318-DH768	Schematic Geological Section
②	Fig 2-2-15	DH667-DH475	Schematic Geological Section
③	Fig 2-2-16	DH318-DH466	Detailed Section of Ore Horizon
④	Fig 2-2-17	DH667-DH461	Detailed Section of Ore Horizon
⑤	Fig 2-5-2	DH525-DH252	Detailed Geological Section
⑥	Fig 2-5-3	DH263-DH122	Detailed Geological Section
⑦	Fig 2-5-4	DH73-DH776	Detailed Section of Ore Horizon
⑧	Fig 2-5-6	DH453-DH45	Detailed Geological Section
⑨	Fig 2-5-7	DH421-DH475	Detailed Geological Section
⑩	Fig 2-5-8	DH812-DH43	Detailed Section of Ore Horizon
⑪	Plate 1-1~Plate 1-4	DH603-DH695	Schematic Geological Section
⑫	Plate 2	DH629-DH775	Schematic Geological Section
⑬	Plate 3-1~Plate 3-2	DH629-DH775	Detailed Section of Ore Horizon
⑭	Plate 4-1~Plate 4-2	DH374-DH590	Detailed Section of Ore Horizon
⑮	Plate 5	DH79-DH682	Detailed Section of Ore Horizon
⑯	Plate 6	DH159-DH363	Detailed Section of Ore Horizon
⑰	Plate 7-1~Plate 7-2	DH314-DH372	Detailed Section of Ore Horizon
⑱	Plate 8	DH729-DH95	Detailed Section of Ore Horizon

Fig. 2-2-13 Index Map of Geological Sections

SCHEMATIC GEOLOGICAL CROSS-SECTION - 153

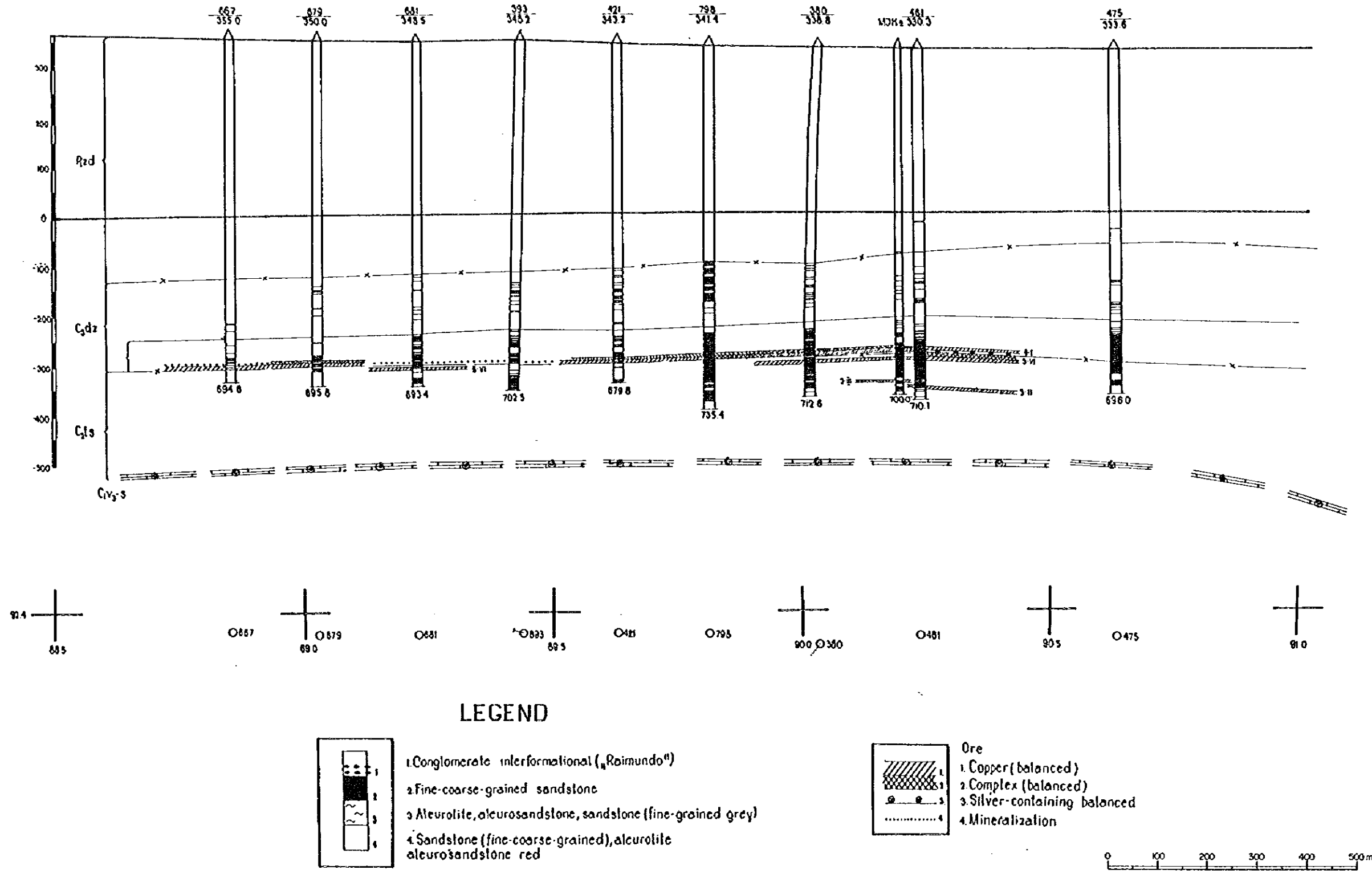


Fig. 2-2-15 Schematic Section of the Central Orebody in the Zhaman-Aibat Ore Deposit (along the line DH667-DH475)

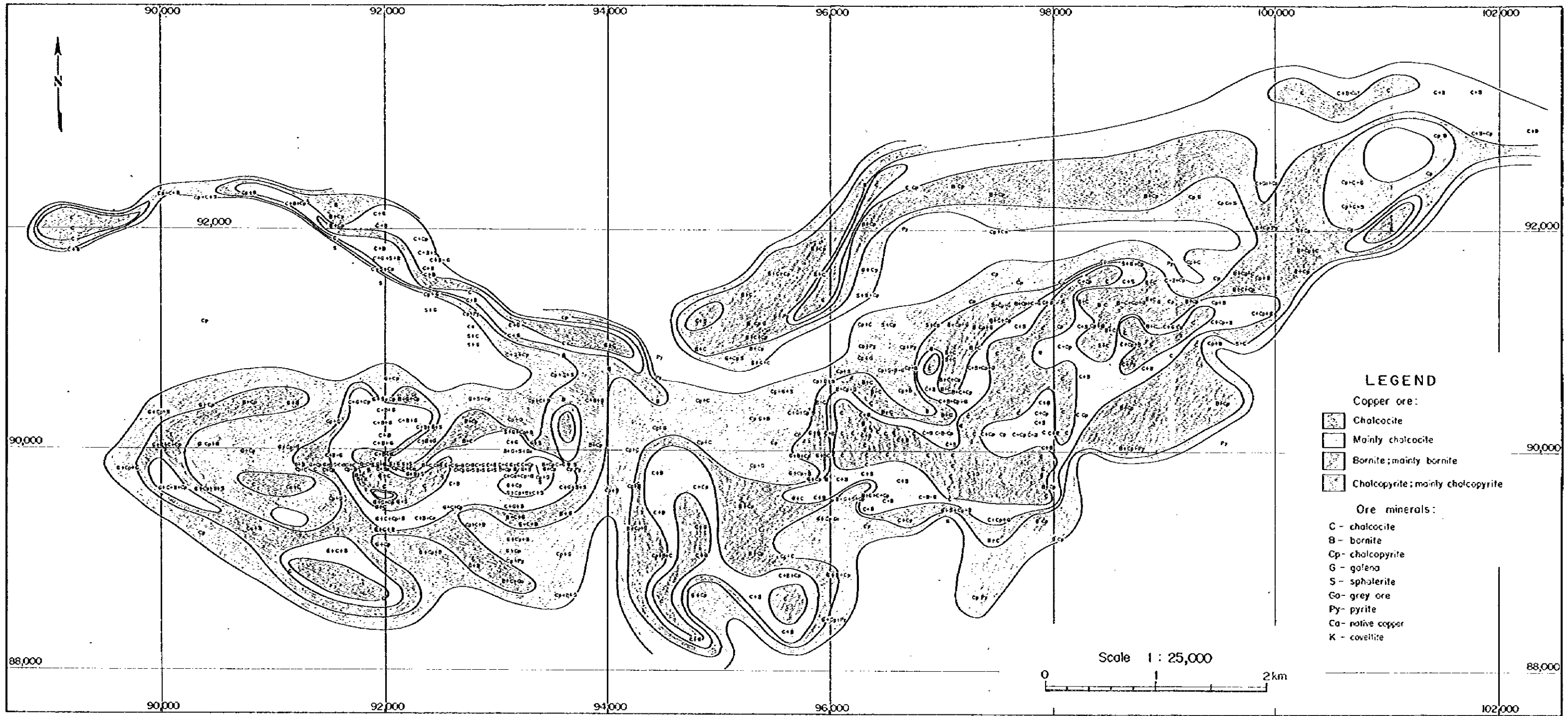


Fig. 2-2-18 Copper Mineral Assemblage of the Zhāman-Aibat Ore Deposit



Table 2-2-3 General Character of the Eastern, Central and Northern Orebody

Orebody		Eastern Orebody	Central Orebody	Northern Orebody
Ore Horizon	Main Minor	4-I 3-V ~ VI, 4-II ~ III	4-I 3-V ~ VI, 4-II ~ III	4-I 3-V ~ VI
Ore Type		mainly Copper Ore	Complex Ore and Copper Ore	mainly Copper Ore
Ore Minerals	Common	chalcocite, digenite djurleite, bornite	chalcocite, digenite djurleite, bornite	chalcocite, digenite djurleite, bornite
	Rare	chalcopyrite galena sphalerite	chalcopyrite galena sphalerite	chalcopyrite native silver electrum
	Very Rare	native silver electrum	native silver	galena sphalerite
Ore Reserve*		116 million tons	38 million tons	39 million tons
Thickness (average)*		5.5m	4.6m	6.6m
Depth		470m - 650m	620m - 650m	550m - 710m
Ore Grade* (average)	Cu	1.3%	Complex Ore 1.5% Copper Ore 1.9%	1.3%
	Pb	-	1.8%	0.1%
	Zn	-	0.3%	-
	Ag	11g/t	11g/t	37g/t

\*: geological resources (see chapter 3)

## Chapter 3 Geological Resources Estimation

### 3-1 Data Base

The number of drill holes and total drill length have reached 1,006 holes and 638,587.4m, respectively (Table 2-1-1). A Drilling pattern of 200m x 200m and 400m x 400m grid spacing as in the former USSR system, has been adopted. In the Eastern and Central Orebody a 100m x 200m grid spacing has been partially practiced (Fig.2-1-1). Core recovery has reached greater than 90% of entire drill hole length and 95% in the mineralized zones. The core is cut using a core splitter and one half of the core of 0.3m - 1.0m in length is used for assay. Specific Gravity (SG) is measured before the chemical assay by the Zhezkazgangeologiya, and is determined to be 2.60 for the deposit.

The assay laboratory, analytical methods and detection limits on each element are as follows;

Elements	Laboratory	Method	Detection limit
Cu	A. O. Zhezkazgangeologiya	Atomic absorption	0.01%
Pb	A. O. Zhezkazgangeologiya	Atomic absorption	0.01%
Zn	A. O. Zhezkazgangeologiya	Atomic absorption	0.01%
Ag	A. O. Karagandageologiya	Atomic absorption	0.1 g/ton
Re	A. O. Karagandageologiya	Radioactivation	0.01 g/ton
S	A. O. Zhezkazgangeologiya	Atomic absorption	0.01%

Chemical contents of Cu, Pb, Zn and Ag were determined on each split sample, but Re and S were assayed on the composite samples. Therefore the accuracy of assay results is quite different between Cu, Pb, Zn and Ag group and Re and S group.

In order to confirm validity of the chemical assay data, a total of 36 check samples were selected and re-analyzed in a Canadian laboratory by the atomic absorption spectrometry assay method. The assay results are summarized in Appendix 7, and 36 pairs of assay results in two scatter plots of both Cu (%) and Ag (g/t) are shown in Fig.2-3-1 and Fig.2-3-2. The correlation between copper results obtained by the Zhezkazgangeologiya Laboratory and by the Canadian laboratory is very high with a correlation coefficient of 0.996. Silver assay results are somewhat erratic and the silver correlation is lower than that of copper, but is still as high as 0.938. Overall trends of copper and silver are coincident and are regarded as satisfactory. The assay results from the two laboratories was also checked by a Japanese laboratory and are in agreement.

For the geological resources estimation, construction of the Zhaman-Aibat Deposit data base was started in 1995, and completed in 1996. Input parameters to this data base are ;

- a) Locality (E-W coordination, N-S coordination)
- b) Elevation
- c) Inclination (Inclination, Azimuth)
- d) Depth of samples
- e) Assay data (Cu, Pb, Zn, Ag, Re, S)
- f) Ore horizon

Details of the data base structure are shown in Table 2-3-1.



**Table 2-3-1 Data Base Used for the Estimation of Geological Resources  
in the Zhaman-Aibat Ore Deposit**

<b>Drill holes</b>	<b>Total number</b>	: 800
	<b>Location</b>	Range of E-W coordination : 85,000 - 105,000 Range of N-S coordination : 86,700 - 94,700
	<b>Data base item</b>	: Drill hole No., E-W coordination, N-S coordination, Elevation Drill length, Inclination, Azimuth
<b>Samples</b>	<b>Total number</b>	: 7,897
	<b>Data base item</b>	<b>Location</b> : Depth (from,to), Sample length <b>Assay elements</b> : Cu, Pb, Zn, Ag, Re, S <b>others</b> : Ore horizon

### 3-2 Basic Statistics

The statistical characteristics of 7,897 chemical assay data on each element, namely Cu, Pb, Zn, Ag, Re, are summarized in Table 2-3-2 and log probability plots of each element are shown in Fig.2-3-3.

The log probability plot of Cu assays confirms that a discontinuity exists at around 0.2% Cu. In grades higher than 0.2% Cu, the distribution tends towards a lognormal distribution but in lower than 0.2% Cu they show an erratic distribution. A similar discontinuity could be seen in the distributions of other elements, such as Pb, Zn, Ag, Re. The erratic distribution at the interval between the detection limit and the discontinuity suggests that the reliability of chemical assay in these intervals is very low and these data should be eliminated from the data analysis.

The results in the form of a correlation matrix for each element are shown in Table 2-3-2. The result of the correlation analysis between Cu (%) and Ag (g/t) shows clear positive correlation and the correlation coefficients were calculated as 0.6. No other clear correlation coefficients could be seen.

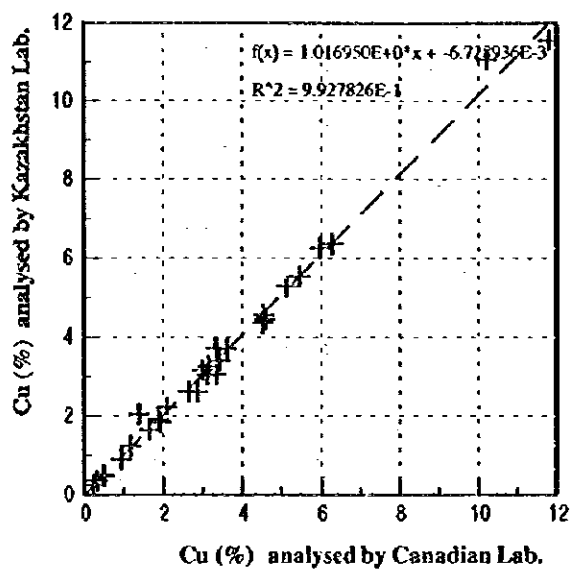


Fig.2-3-1 Scatter Plot of Cu Check Analysis of Ore Samples from Zhaman-Aibat Are (Canadian Lab vs Kazakhstan Lab)

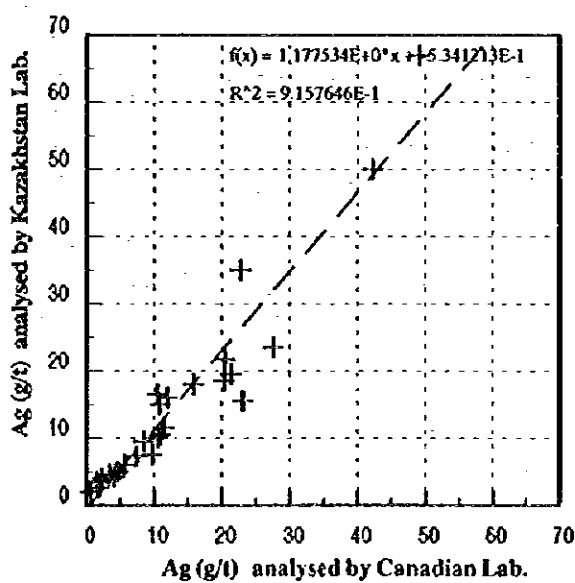


Fig.2-3-2 Scatter Plot of Ag Check Analysis of Ore Samples from Zhaman-Aibat Are (Canadian Lab vs Kazakhstan Lab)



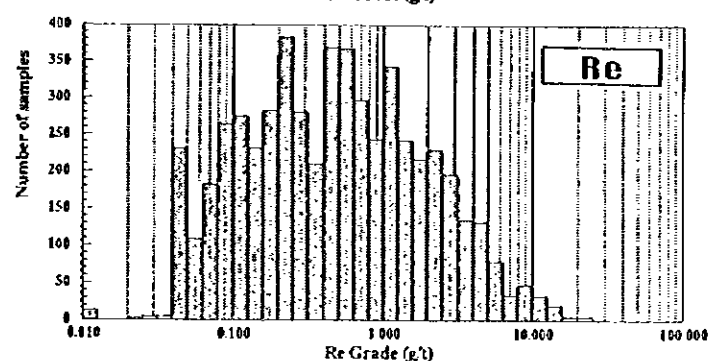
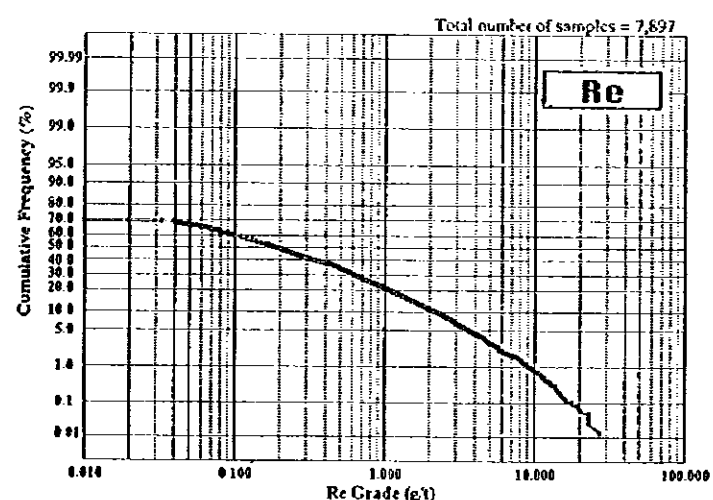
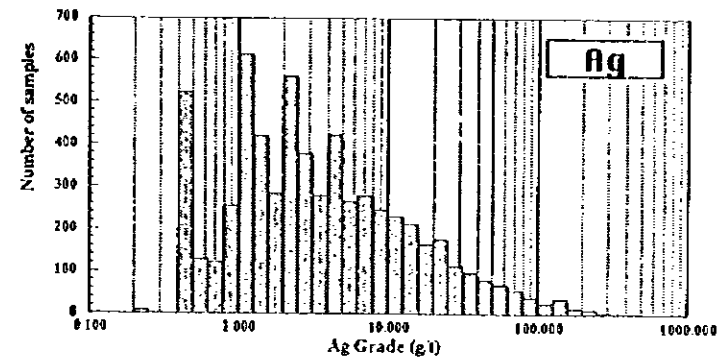
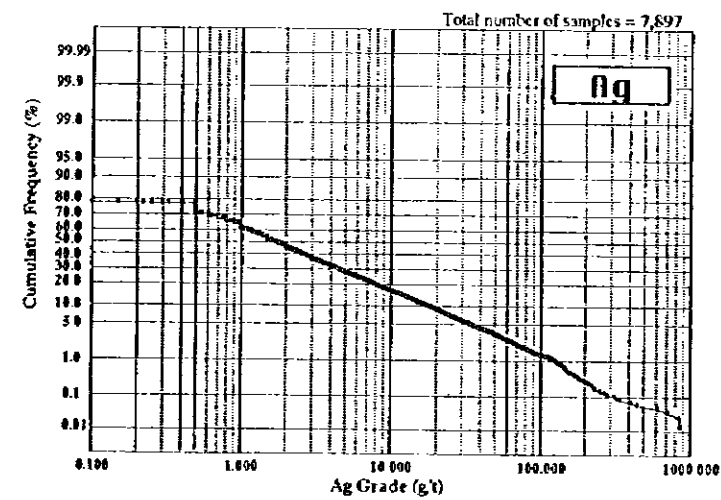
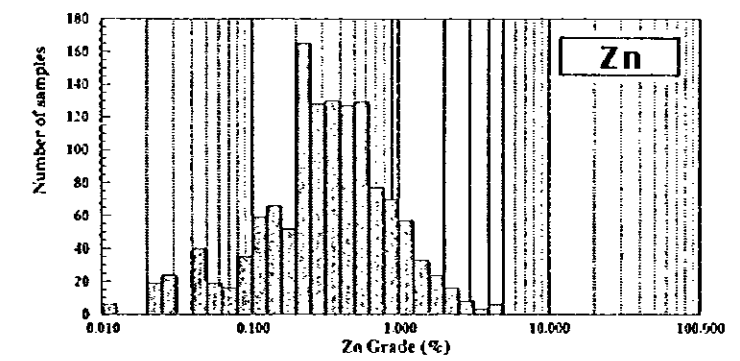
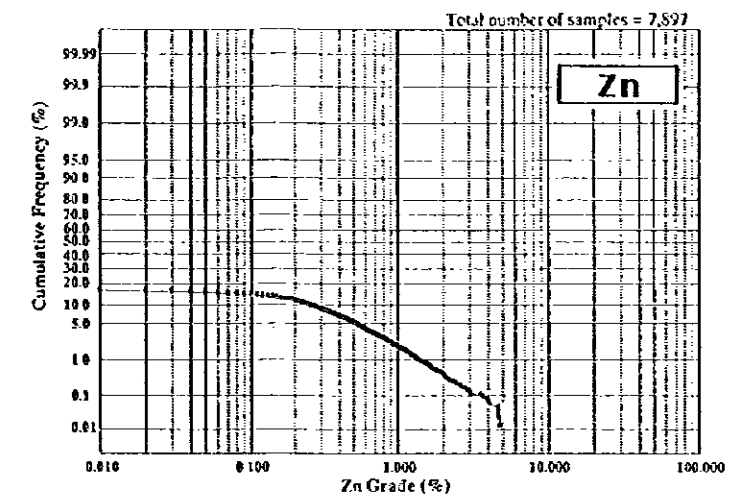
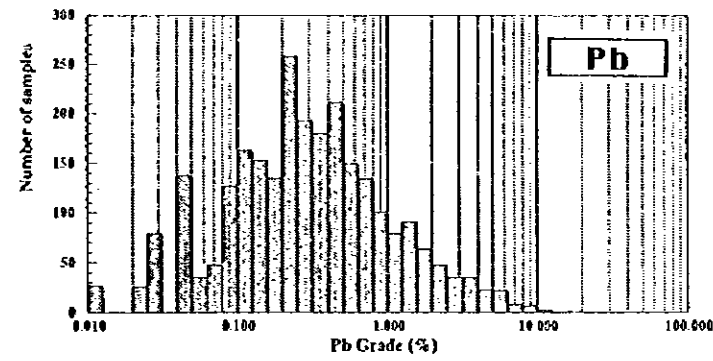
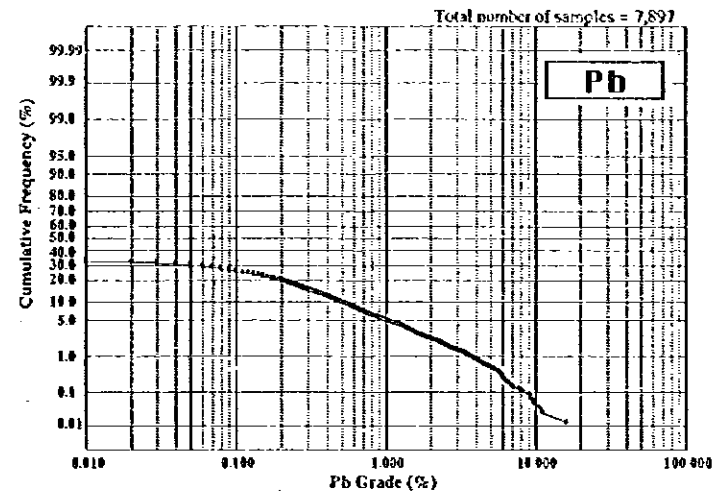
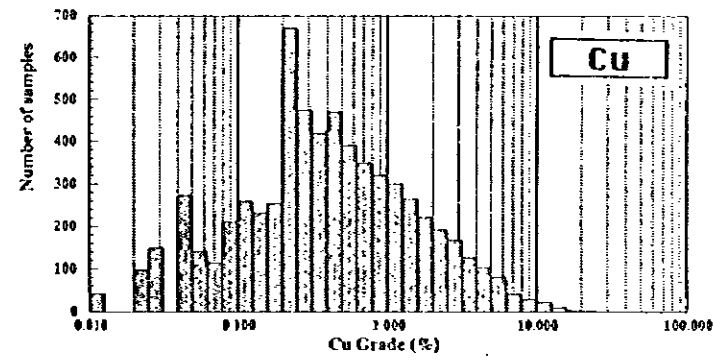
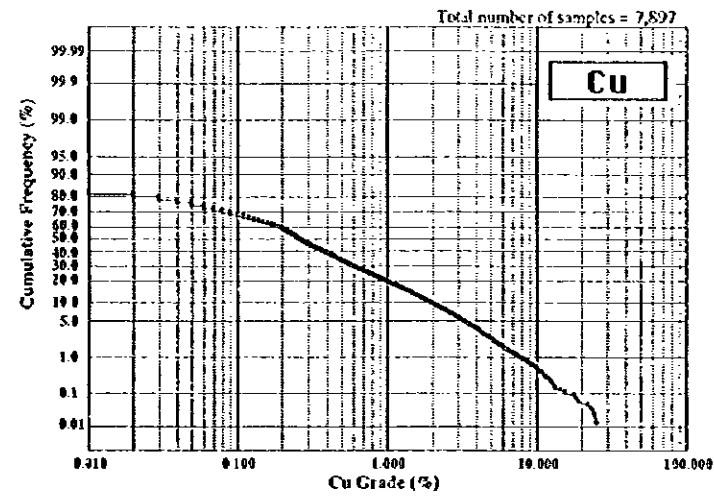


Fig.2-3-3 Probability Plots of Cu, Pb, Zn, Ag and Re Assays  
(Total Number of Samples = 7,897)

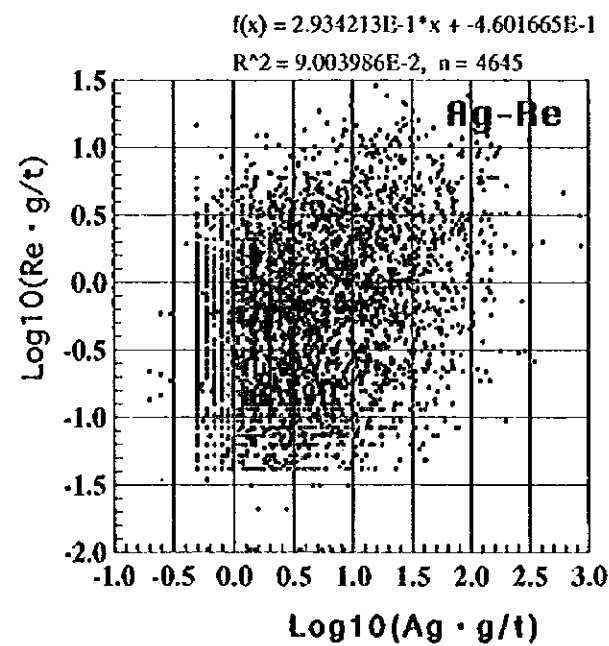
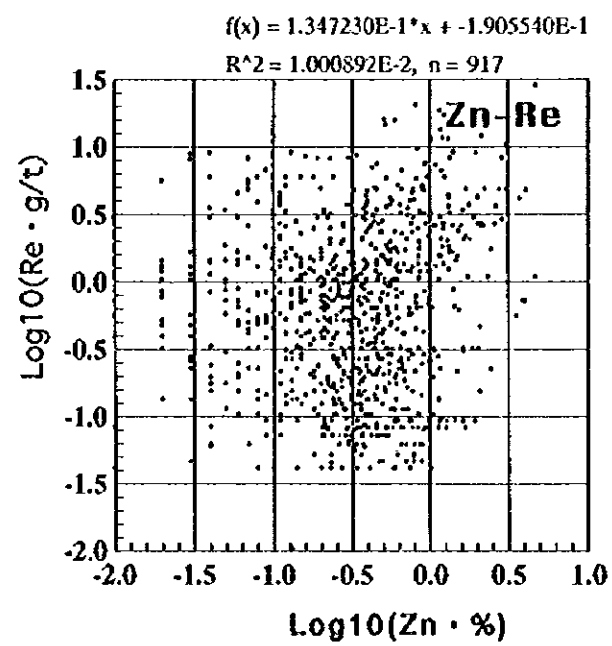
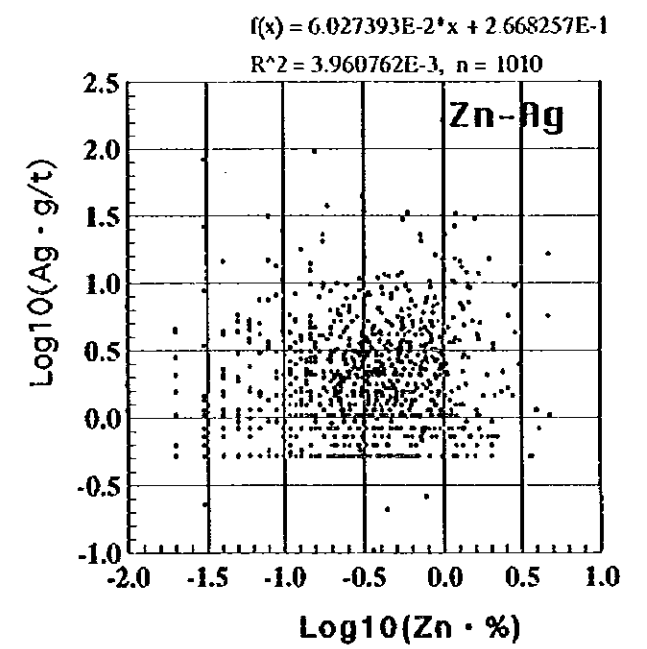
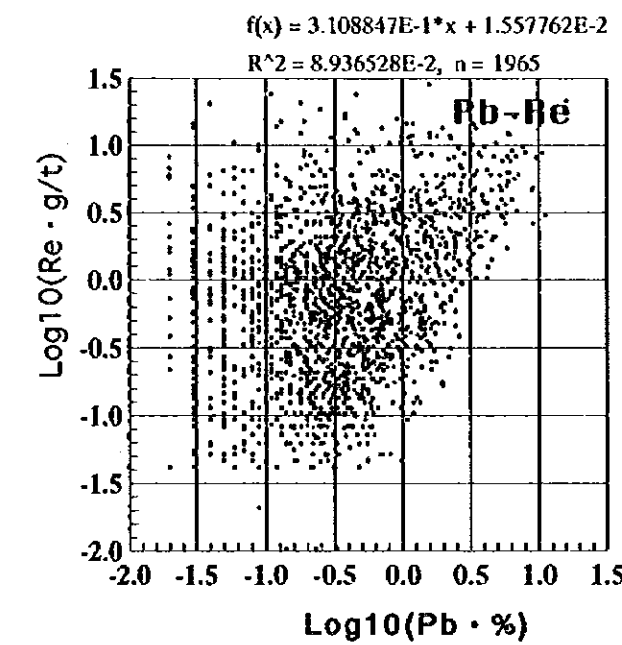
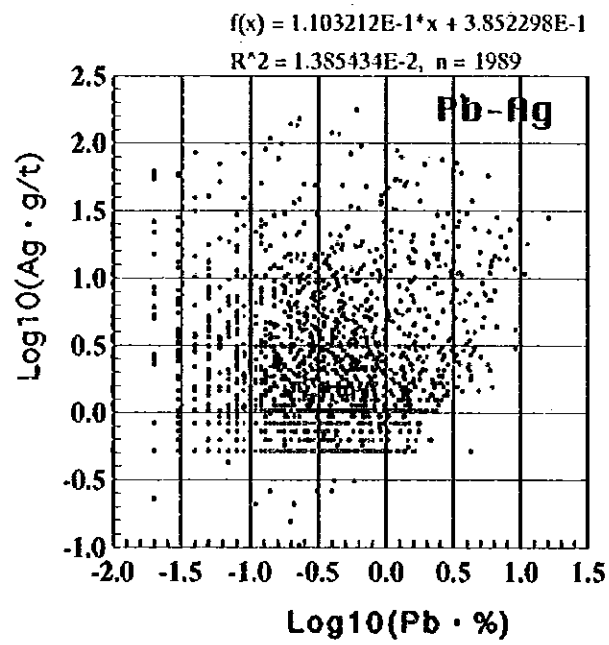
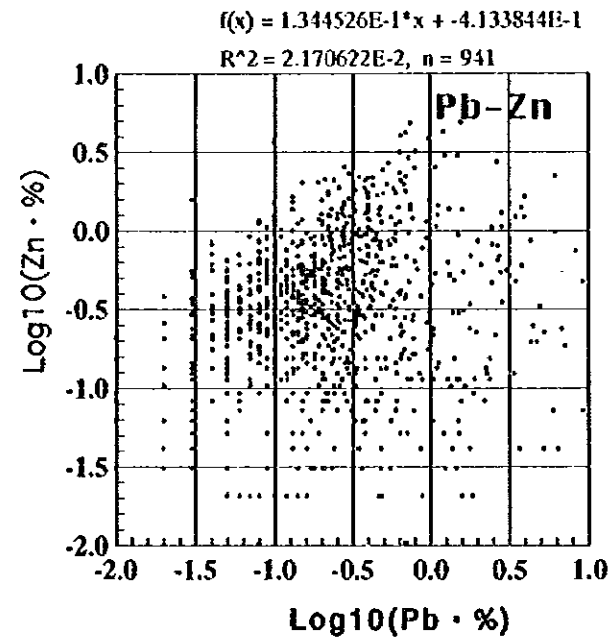
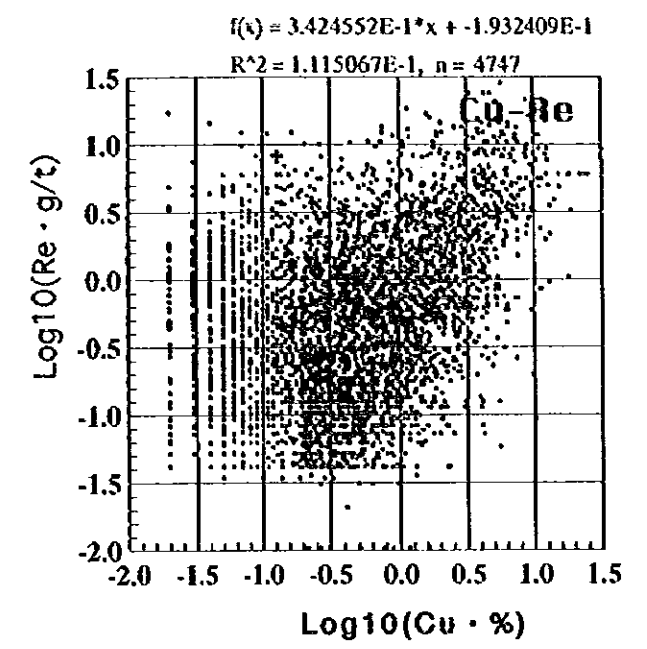
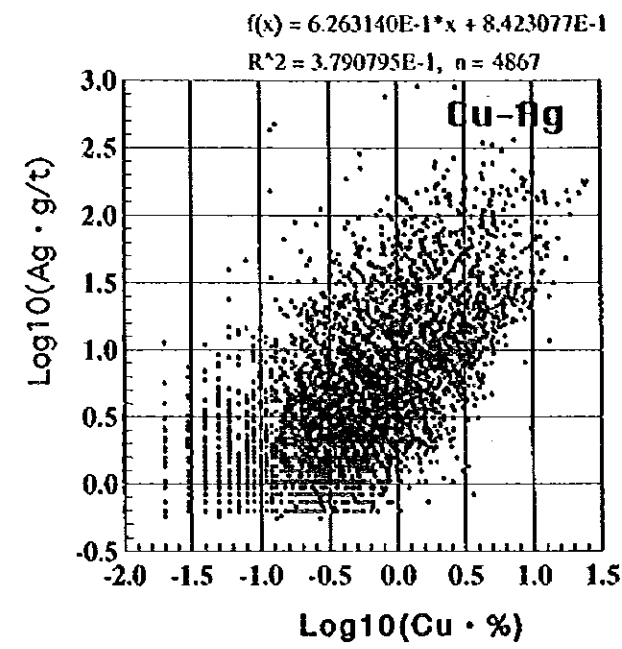
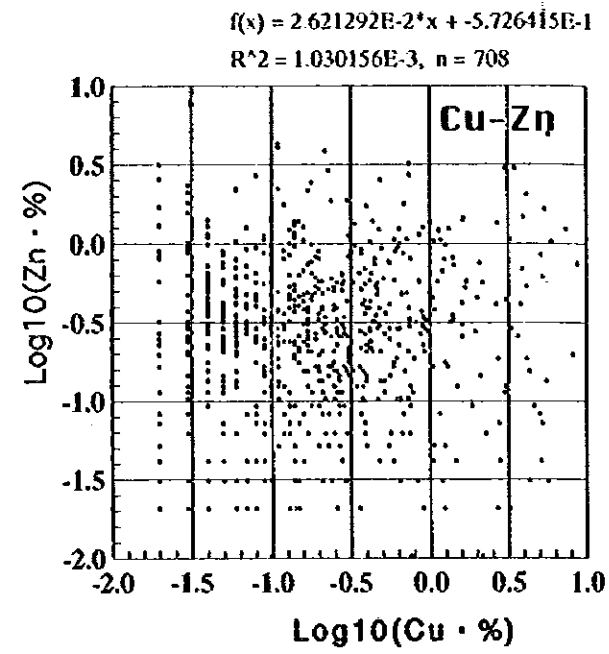
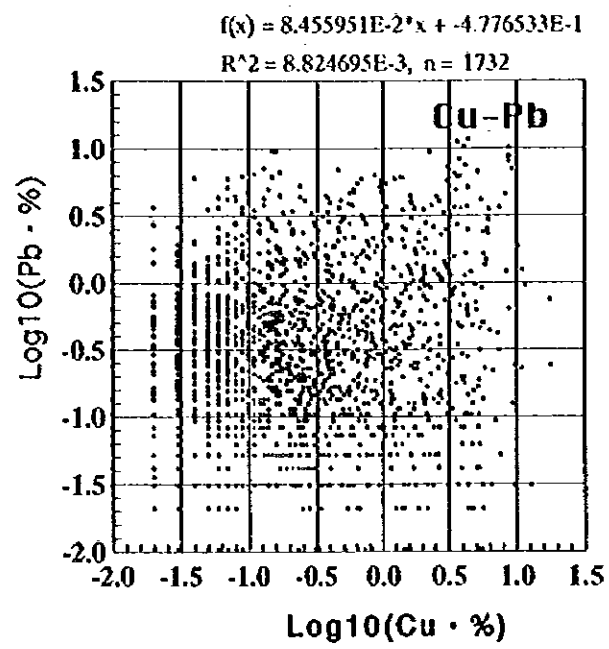


Fig.2-3-4 Correlation Diagrams between Element's Pair



Table 2-3-2 Basic Statistics of the Ore Samples from the Zhaman-Aibat Ore Deposit

Statistics	Cu (%)	Pb (%)	Zn (%)	Ag (g/t)	Re (g/t)	S (%)
Maximum	25.50	16.24	4.82	868.0	27.56	46.40
Minimum	<0.01	<0.01	<0.01	<0.1	<0.01	<0.01
Median	0.26	0.01	0.01	1.7	0.18	0.27
Average	0.17	0.02	0.01	0.8	0.12	0.12
Average+1 $\sigma$	1.40	0.14	0.05	15.6	1.27	1.24
Average- $\sigma$	0.02	0.00	0.00	0.0	0.01	0.01

Table 2-3-3 Correlation Matrix, Zhaman-Aibat Ore Deposit

	Cu	Pb	Zn	Ag	Re	
<b>Cu</b>		1732 2.58	708 2.58	4867 2.58	4747 2.58	← number of samples ← t-value, t(f,0.005)
<b>Pb</b>	0.094 3.92		941 2.58	1989 2.58	1965 2.58	
<b>Zn</b>	0.032 0.85	0.147 4.56		1010 2.58	917 2.58	
<b>Ag</b>	0.616 54.50	0.118 5.28	0.063 2.00		4645 2.58	
<b>Re</b>	0.334 24.40	0.299 13.88	0.100 3.04	0.300 21.43		← coefficient of correlation ← t-value, calculated

Table 2-3-4 Ore Classification and Cut Off Grade for the Geological Resources Estimation of the Zhaman-Aibat Ore Deposit

	Cu (%)	Pb+Zn (%)	Thickness (m)
<b>Cu Ore</b>	$0.40\% \leq \text{Cu}$	$\text{Pb}+\text{Zn} < 0.80\%$	$3\text{m} \leq \text{Thickness}$
<b>Complex Ore</b>	$0.30\% \leq \text{Cu}$	$0.80\% \leq \text{Pb}+\text{Zn}$	$3\text{m} \leq \text{Thickness}$
<b>Pb-Zn Ore</b>	$\text{Cu} < 0.30\%$	$1.10\% \leq \text{Pb}+\text{Zn}$	$3\text{m} \leq \text{Thickness}$
<b>Cu Ore</b>	$1.20\% \text{m} \leq \text{Cu} \times \text{Thickness}$	$(\text{Pb}+\text{Zn}) \times \text{Thickness} < 2.40\% \text{m}$	$\text{Thickness} < 3\text{m}$
<b>Complex Ore</b>	$0.90\% \text{m} \leq \text{Cu} \times \text{Thickness}$	$2.40\% \text{m} \leq (\text{Pb}+\text{Zn}) \times \text{Thickness}$	$\text{Thickness} < 3\text{m}$
<b>Pb-Zn Ore</b>	$\text{Cu} \times \text{Thickness} < 0.90\% \text{m}$	$3.30\% \text{m} \leq (\text{Pb}+\text{Zn}) \times \text{Thickness}$	$\text{Thickness} < 3\text{m}$

### 3-3 Calculation Methods

The Eastern Orebody and the main part of the Central Orebody were selected for the geological resources estimation in the first and second year's studies. For the third year's study, the overall geological resources of the Zhaman-Aibat Deposit were estimated.

The polygon method was utilised for the estimation. The procedure of the estimation is summarized below :

(1) The basic data, such as depth, thickness, assay results and ore horizon were input to the data base both by the Japanese survey team and by the Zhezkazgangeologiya. Only 4-I Horizon data were selected for the calculation.

(2) The mineralized layers were calculated and categorized into three types of ore according to their major chemical characteristics. They are 1) Copper Ore, 2) Complex Ores, and 3) Lead-Zinc Ores. The cut-off grade for each ore type was determined, according to the resolution of the Zhezkazgangeologiya and of the State Committee for Reserves of the State Committee for Geology of the Republic of Kazakhstan. The cut-off grades were set at 0.4% Cu for the copper ores, 0.8%Pb+Zn and 0.3%Cu for the complex ores, 1.1%Pb+Zn for the lead-zinc ores. (Table 2-3-4).

(3) In case of the presence of interbands of waste between ore layers and the accumulated thickness does not exceed 4 meters, and the weighted average grade of ore is higher than the cut-off grade, the zone will be determined to be ore not waste.

(4) A cut-off thickness of ore is incorporated in the determination of ore/waste. Even if the thickness of ore is less than 3 meters and the grade of ore is high, determination of ore/waste will be made by referring to the value of ore thickness(m) x ore grade(%).

(5) Ore blocks were constructed by the polygon method. The ore reserves and metal amount were calculated on each polygon block. The average specific gravity was assumed as 2.600 which is the same value used by the Zhezkazgangeologiya.

(6) The calculated ore reserves of each polygonal block were categorized into three groups on the basis of exploration stage, and were correlated to the following ore reserve categories:

- a) Category I; drill pattern is denser than 200m x 200m grid, and continuity (of ore blocks) is confirmed.
- b) Category II; drill pattern is not denser than 200m x 200m grid, and continuity is confirmed.
- c) Category III; drill pattern is not denser than 200m x 200m grid, and no continuity is confirmed.

In this report, the geological resources are defined as the total amount of the ore reserves of Category I and Category II. In the former USSR system, Category A and Category B correspond to Category I and Category II respectively.



### 3-4 Results of Calculation

The results of the geological resources estimation are shown in Table 2-3-5, Fig.2-3-5 and Fig.2-3-6.

The geological resources is calculated as ;

**Eastern Orebody:** 116 million tons (mainly Cu Ore: 1.3%Cu, 11g/tAg, 5.5m thick),  
**Central Orebody:** 38 million tons (Cu Ore: 1.9%Cu, 11g/tAg, 3.9m thick,  
Complex Ore: 1.5%Cu, 1.8%Pb,0.3%Zn, 11g/tAg, 5.6m thick),  
**Northern Orebody:** 39 million tons (mainly Cu Ore: 1.3%, 37g/t Ag, 6.6m thick),  
**Total:** 193 million tons (1.4%Cu, 0.3%Pb, 16g/tAg, 5.4m thick)

87.4% of the whole geological resources are Copper Ore, and 10.9% are Complex Ore. Lead-Zinc Ore account for only 1.7% of the geological resources. The zinc grade is calculated as 0.3% in the Complex Ore of the Central Orebody. It can be seen that zinc is not an important factor for the evaluation of the Zhaman-Aibat Deposit.

The Copper Ore is widely distributed in the Zhaman-Aibat Deposit, but the Complex Ore and the Lead-Zinc Ore show uneven distributions. 85% of the Complex Ore and 65% of the Lead-Zinc Ore are in the Central Orebody.

In recent years, the Zhezkazgangeologiya calculated the total amount of Copper Ore and Complex Ore in the Zhaman-Aibat Deposit. They estimated that the total ore reserves were 190 - 200 million tons (1.6%±Cu, 0.25%±Pb, 18g/t±Ag). Compared with the results of the Japanese survey team, it can be seen that the copper grade is a little higher. But there is no serious problem in this stage of geological resources estimation.

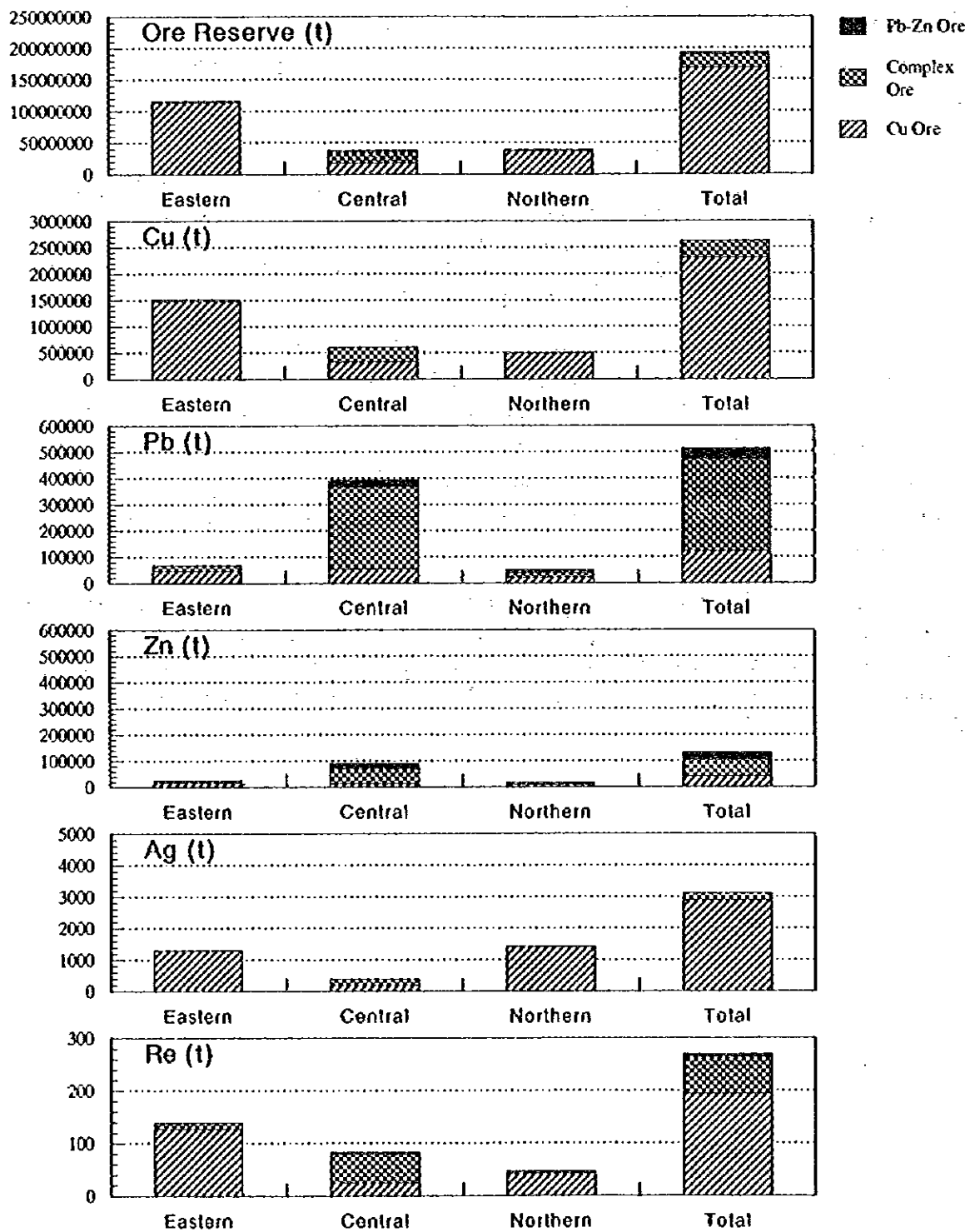


Fig.2-3-6 Geological Resources of the 4-t Horizon of the Zhama-Aibat Ore Deposit (Category I + Category II)







## **Chapter 4 Remote Sensing Data Analysis**

### **4-1 Remote Sensing Data**

The analysed satellite data are from two scenes of Landsat TM shown in Fig.2-4-1. Satellite images used for the photogeological analysis are two false color images; one scene is a band combination of 1(blue), 4(green) and 5(red), the other is a combination of 4(blue), 5(green) and 7(red). The digital data of six bands of 1,2,3,4,5 and 7 were used for the digital data processing for the extraction of alteration zones.

### **4-2 Method**

#### **4-2-1 Photogeological Analysis**

For the geologic interpretation by photogeological methods it is necessary to identify the photogeologic parameters and factors and to translate these factors to geographic, botanic and geologic phenomena. Because the satellite image used in this analysis has no stereographic image, the topography, water system, geology, structural geology, alteration and so on were interpreted by single photogeological observations.

In the analysis the following factors were observed, extracted and analyzed.

- (1) Photogeological character
  - Color classification
  - Texture (very fine, fine, medium, rough)
- (2) Analysis of topographic parameters
  - Water system (pattern, density and others)
  - Topographic pattern
  - Structural topography (degree of stratification)
- (3) Analysis of geological structure
  - Strata and folding (inclination, strike)
  - Fault and lineament (relation of crossing, sense)
  - Ring, basin and other structures
- (4) Analysis of geology
  - Surface texture classification (rock faces)
  - Similar surface distribution (distribution of a rock type)
  - Geologic unit classification
  - Alteration zone

For the photogeologic observation and interpretation of these factors in the satellite image, the following parameters were adopted to analyze each factor; (Note: the effect or influence of vegetation was rather weak in the satellite images in this area).

The distinguishing parameters obtained from photogeological observation are hue, lightness,

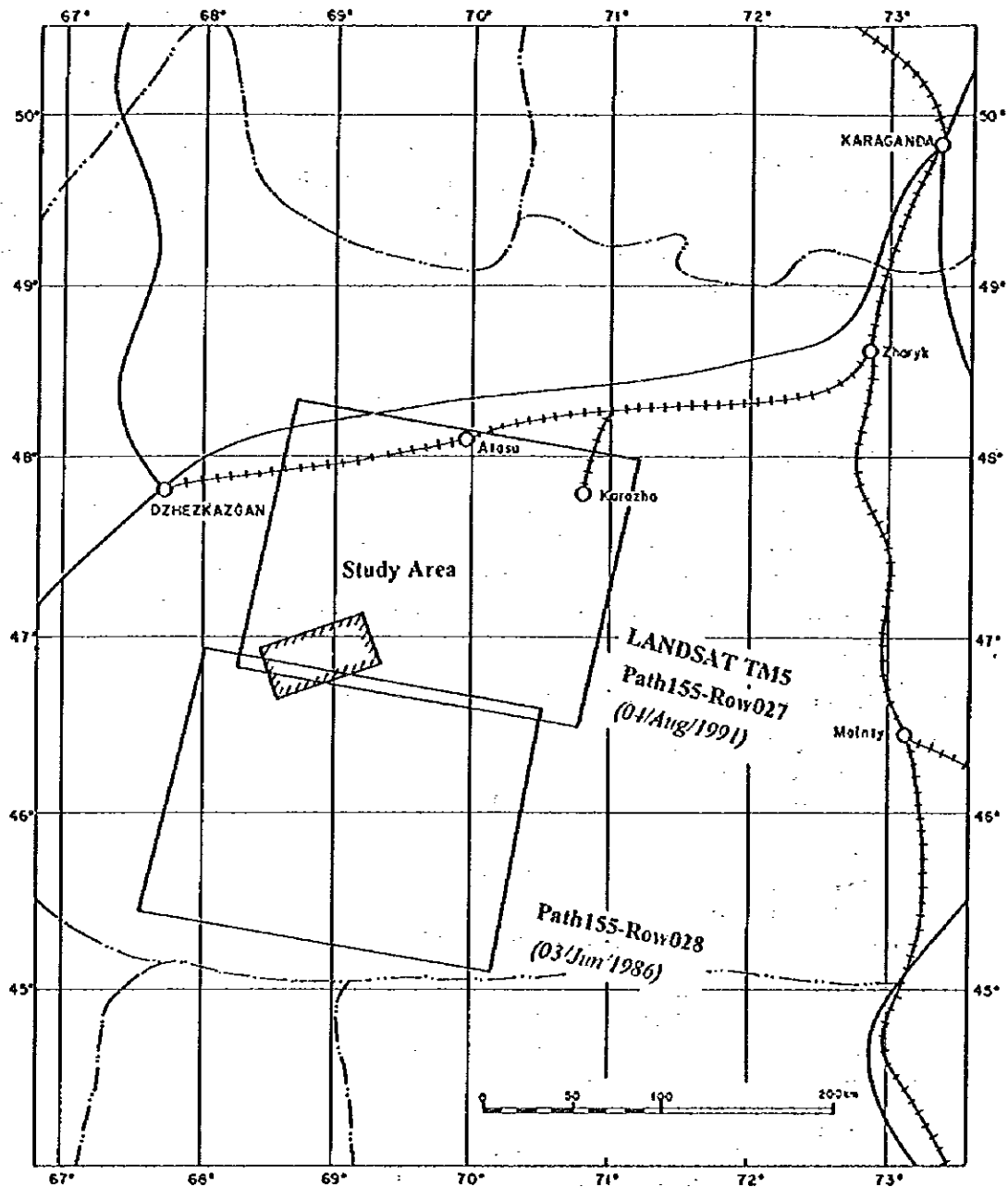


Fig.2-4-1 Location Map of Satellite Image Analysis in the Zhaman-Albat Area

shade, texture, pattern, form, size and others. Photogeological observation was carried out to observe these parameter individually or in combination.

Of these parameters, hue is the most important and useful parameter and when combined with lightness it is effective in detecting regions of similar rock type. In fact the combination of hue, lightness and saturation (chroma) in the analysis is a very powerful method to identify similar rock types. In the case of satellite images the hue is that of false color, and by selection of suitable combinations of each color band precise interpretation for recognition of a particular target is possible.

The lightness is the most primitive parameter used to detect regions containing the same characteristic. Even if the photograph is mono-chrome, lightness provides much information; for example, it is useful in interpreting the inclination of a plane (surface) in the topography.

The texture of the surface is basically the reflection of minute (infinitesimal / microscopic) changes (variation/transition) in the image, and if the frequency is below the limit of detection for the observer the change is observed as smoothness in the image as the class of coarse (or rough) to fine-grained. And the dimension of frequency to repeat gives the different pattern information as uneven, smooth, (equi-and unequi-)granular to the observer.

In satellite images, the photograph is an accumulated image of pixel data, therefore the texture precision (pitch/size) depends on its resolution and on the minimum size of frequency pitch is the same as the unit pixel size. The smaller data is buried in a single pixel and cannot be detected in such a case.

The pattern parameter is a larger scale phenomenon reflecting the larger, regularly repeated arrangement on the ground surface. One of the most common patterns is a lineament which can be classified as straight, curved or meandered, and by its length, and in combination they can be classified as parallel, radial, crossing (at right angles, oblique, rectangle, grid, network), circular (concentric), arborescent or irregular/random arrangement. Especially for the interpretation of eroded topography pattern of water courses and others carved (engraved) on the surface, the parameter of pattern is the most important factor. Patterns of vegetation or artificial structures (building, road, plant, farm, afforestation and others) also cannot be regretted in interpretation.

Vertical enhancement by the effect of shade (shadow) is an important parameter for topographic analysis. This information comes not only from the uneven surface of the ground but also from the difference of vegetation, water content (saturation/porosity) of the vegetation or underground geological structure or rock faces in some case. It was therefore an important parameter for this photogeological analysis especially in the absence of stereographic information of satellite images.

The size parameter can be used with each parameter described above. By the measurement of size some useful information can be derived. For example, the thickness of water course indicates the porosity of rock or soil and/or composing grain size.

By combining these parameters the photogeological observation and interpretation effectively provided information about topography, water system, geologic structure, geology and stratigraphy.



## 4-2-2 Satellite Image Data Processing

Satellite data from Landsat TMS scenes (Path 155, Row 027 and Path 155, Row 028) were used for the satellite image analysis. An analysis area was selected as a subscene contained within the two scenes and including the Zhaman-Aibat area. Image processing and analysis were carried out on a VAX6310 (DEC) computer using the DeAnza IP9527 (DOULD) owned by Sumitomo Metal Mining Company.

The spectral data are as follows; bands 1, 2, and 3 are in the visible region, band 4 is centered at 0.85 micro.m, band 5 is centered at 1.6 micro.m, band 7 is centered at 2.2 micro.m, and band 6 is in the thermal region.

### (1) False color composite image

False color composite images are made up of three bands in combination selected from seven TM bands. Composite images are as follows;  
Red, Green, Blue: band 4, band 3, band 2  
Red, Green, Blue: band 5, band 7, band 1

### (2) Color ratio composite image

A rationing technique between bands is useful to enhance specific characteristics and also to reduce topographic effects. Spectra of clay minerals (kaolinite, illite and montmorillonite) have an absorption feature at a wavelength of approximately 2.2 micro.m that coincides with band 7 of TM. Iron oxide minerals have characteristic spectra in bands of 1, 2, 3, 4 and 7. Generally spectra of iron minerals have weak reflections in band 1, and strong reflections in band 3. It is possible to delineate areas where iron oxide minerals spread on the surface by means of rationing between bands. Composite images are as follows;  
Red, Green, Blue: 5 / 7, 5 / 4, 3 / 1.

### (3) Ratio image with density slice (5/7 and 4/3)

Spectra of clay minerals have weak reflectance in band 7, and strong reflectance in band 5. The ratio 5/7 therefore has high values for clay minerals, resulting in bright tones on the density slice which are assigned red and yellow colors signifying the highest ratio values. But the ratio 4/3 also has high values for vegetation; weak reflectance in band 3, and strong reflectance in band 4. After comparing both ratio images individually, it is possible to distinguish the clay dominant areas from vegetation.

## 4-3 Results of Analysis

### 4-3-1 Results of Photogeological Interpretation

#### Characteristics of topography and water system

The target area was classified into three topographic categories of desert, low plane and low hill (Fig.2-4-2, Fig.2-4-3). For the interpretation, the T.P.C. (1:500,000) map was referred to when necessary. The results of photogeological interpretation are as below:

(1) Desert (Du): The desert area is located at the north-western part of the Zhaman-Aibat target area. It shows yellowish brown in color in the satellite image. (Colors described here are in the

satellite image formed by combination of bands 5,4 and 1, false color). In the desert, dunes developed by the effect of wind are especially distinct in the northern and southern parts in the image. In some places vegetation was detected but water course are rare.

(2) **Low plane (LP):** The low plane is distributed in the area surrounding the desert. Its topographic character is similar to that of desert and at some places it is covered by sand. The vegetation is distinctive and commonly includes "praya" indicating the difference from the desert. The development of "praya" shows the concentrated region of water courses which in this case are run off channels from the hill region.

(3) **Smooth hill (SH):** Smooth hill topography is spread widely and generally it corresponds to altitudes above the desert or low plane. Water courses are developed in the hilly areas but disappear at their margins where water flows into the low planes, and "praya" disappear. Smooth hills show very smooth texture in the image.

(4) **Middle hill (MH):** The middle hill topography extends between the smooth hill and rough hill topography. Its altitude is also between that of the smooth and rough hills. Due to the hard resistant property of its rocks and the developing degree of the stratification it shows a rather rough texture. In geological classification they correspond to units C, D and E.

(5) **Rough hill (RH):** Rough hill topography is located at the central part of the target area, and according to the highly resistant nature of the formations it shows rough texture. It is found at high altitudes and forms a watershed (water divide) with water courses flowing to north and south. Geologically, rough hill areas correspond to the unit of the axial part of the anticline structure.

## **Geology**

By the photogeological analysis the geological classification (corresponding to stratigraphy) of the target area was distinguished as 10 geological units and subunits divided and alphabetically named in ascending order. Referring to published geologic maps (Geologic Map of Kazakhstan, USSR, Scale 1:500,000. and others), these geological units correspond to Carboniferous, Permian, Cretaceous and Quaternary systems. The Carboniferous system described in the maps was not however distinguished in the satellite image.

(1) **Geologic unit A:** The geologic unit A is characteristically shown by the color of dark blue in the satellite image (the color is from the image of false color by band combination of 5,4 and 1. The following description is in the same image). It displays a semi-parallel pattern of water courses has rough texture, is highly resistant and has well developed stratification. It consists of the lowest geologic unit in the target area.

(2) **Geologic unit B:** The geologic unit B shows similar characteristics to unit A. However, it has sparse drainage, smooth texture, medium resistant rocks and the degree of stratification distinguish it from that of unit A. Unit B overlaps unit A, and it is possible to consider that it is a sub-unit of unit A. Unit B occurs in areas surrounding unit A which are widespread in the central part by the area. Unit B is also located in the north-eastern part in an arrangement like a fenster.

(3) **Geologic unit C:** Unit C is characterized by its white color and arborescent drainage pattern, rough texture, medium resistant rocks and very well developed stratification. Its color varies from white to orange, hazy bluish grey and in some parts mozaik texture is observed. Unit C overlays unit B discordantly.

(4) **Geologic unit D:** Unit D is characterized by its color of yellow. Its inclination can be distinguished by its color, and in steeply inclined parts it often shows the topography of cuesta.

(5) **Geologic unit E:** Unit E shows dark blue color, rough texture, medium resistant rocks and in some places is well stratified. Its hue is similar to that of unit A but in the combined image of bands 7, 5, 4 they are clearly different from each other. Unit E is widely spread in the area.

(6) **Geologic unit F:** Unit F was divided into two sub-units. Lower sub-unit F1 has a characteristic bluish grey, color, flat topography, smooth texture and low resistant rocks and differs from the upper unit F2 which shows dark grey and medium resistant rocks. The color tones of both units are rather heterogeneous in all parts of the image, but other characteristic (parameter) are almost the same. These units overlap in many places discordantly.

(7) **Geologic unit G:** Unit G is considered to correspond to Quaternary, and the results of the analysis indicate the sub-unit of Q1, Q2 and Q3. Sub-units Q1 and Q2 are different types of wind-forming strata (dune) and the unit Q3 is "praya".

### Geologic structure

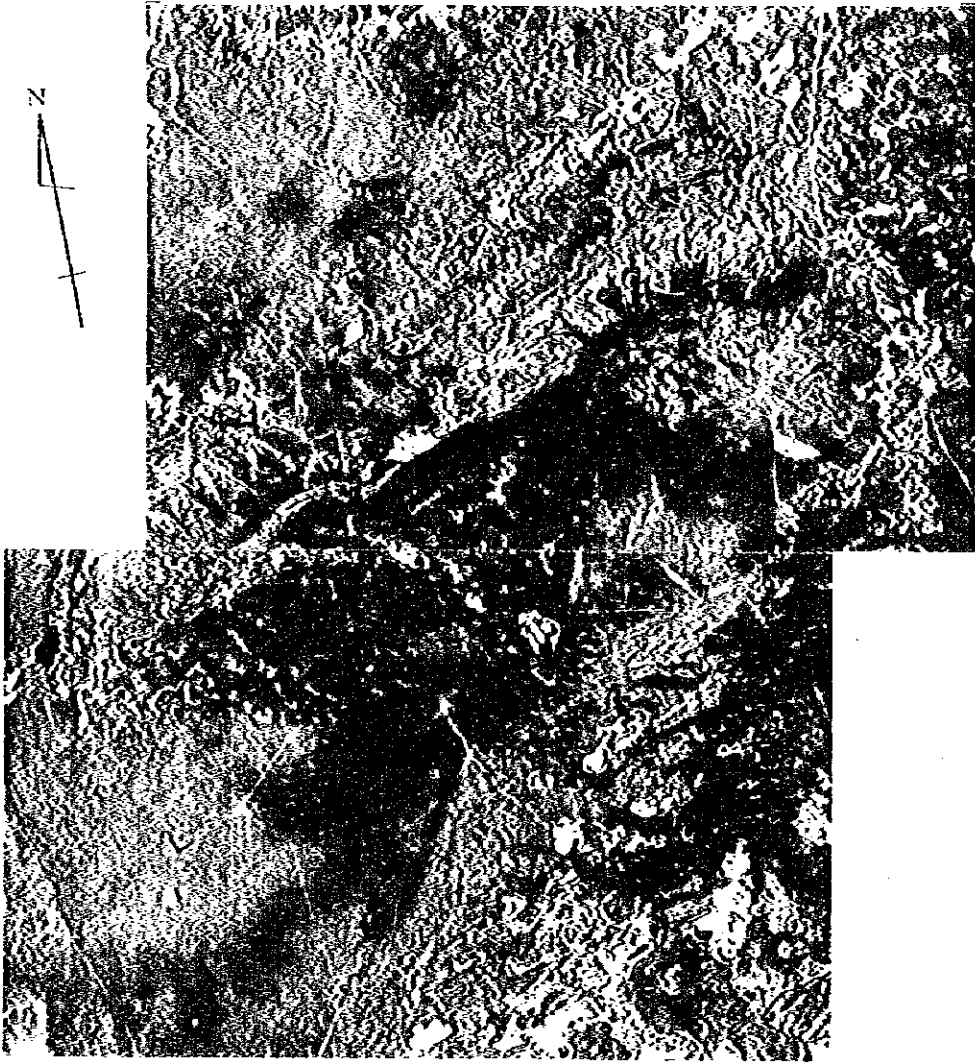
The most important geologic structure in the area is the anticlinal structure located in the central part. Its axis has a direction of east-north-east and plunges to west-south-west. Anticlinal structure is asymmetric with the south wing being more gently sloped than the north wing. The continuity of the axis in the east-northeast direction is cut and shifted by cross faults with north to south strike (direction). Another small anticlinal structure of almost parallel axis was detected to the northeast of this anticline (Fig.2-4-5).

On the contrary faults with meridional strike were detected and they often cut the anticlinal structure described above. Lineaments have no particular dominant direction, but in the north-west part of the area lineaments with north-east direction dominate. Two incomplete circular structures were also detected in the western part of the area.

Table 2-4-1 Geological Interpretation for the Satellite Image Analysis in the Zheman-Albat Area

Geologic Units	Photo Characteristics		Drainage		Rock			Cover		Remarks
	Color	Texture	Pattern	Density	Texture	Resistance	Bedding	Vegetation	Land Use	
Q	white	-	no	-	-	very low	-	no	-	
	light grey	aerial dune	no	-	aerial dune	very low	-	little	-	
	grey	aerial dune	no	-	aerial dune	very low	-	very little	-	
F	dark grey	smooth	dendritic	low	smooth	moderate	poorly	no	-	
	bluish grey	even, smooth	dendritic	low	even, smooth	low	poorly	no	-	
E	dark blue (partially white)	rough	sub-parallel	moderate (partially high)	rough	moderate	partially very well	no	-	
D	yellow	cuesta	sub-dendritic	moderate	cuesta	low	poorly	no	no	
C	white (partially orange)	rough	dendritic	moderate	rough	moderate	very well	no	no	
B	blue	smooth	sub-parallel	low	smooth	moderate	commonly	no	no	
A	dark blue	rough	sub-parallel	high	rough	high	well	no	no	

P155 R027



P155 R028

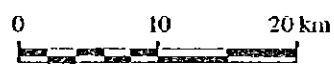


**Fig.2-4-2 False Color Composite of Landsat TM Data for the Zhamen-Albat Area, RGB:571**



# Zhaman - Aibat , Kazakhstan

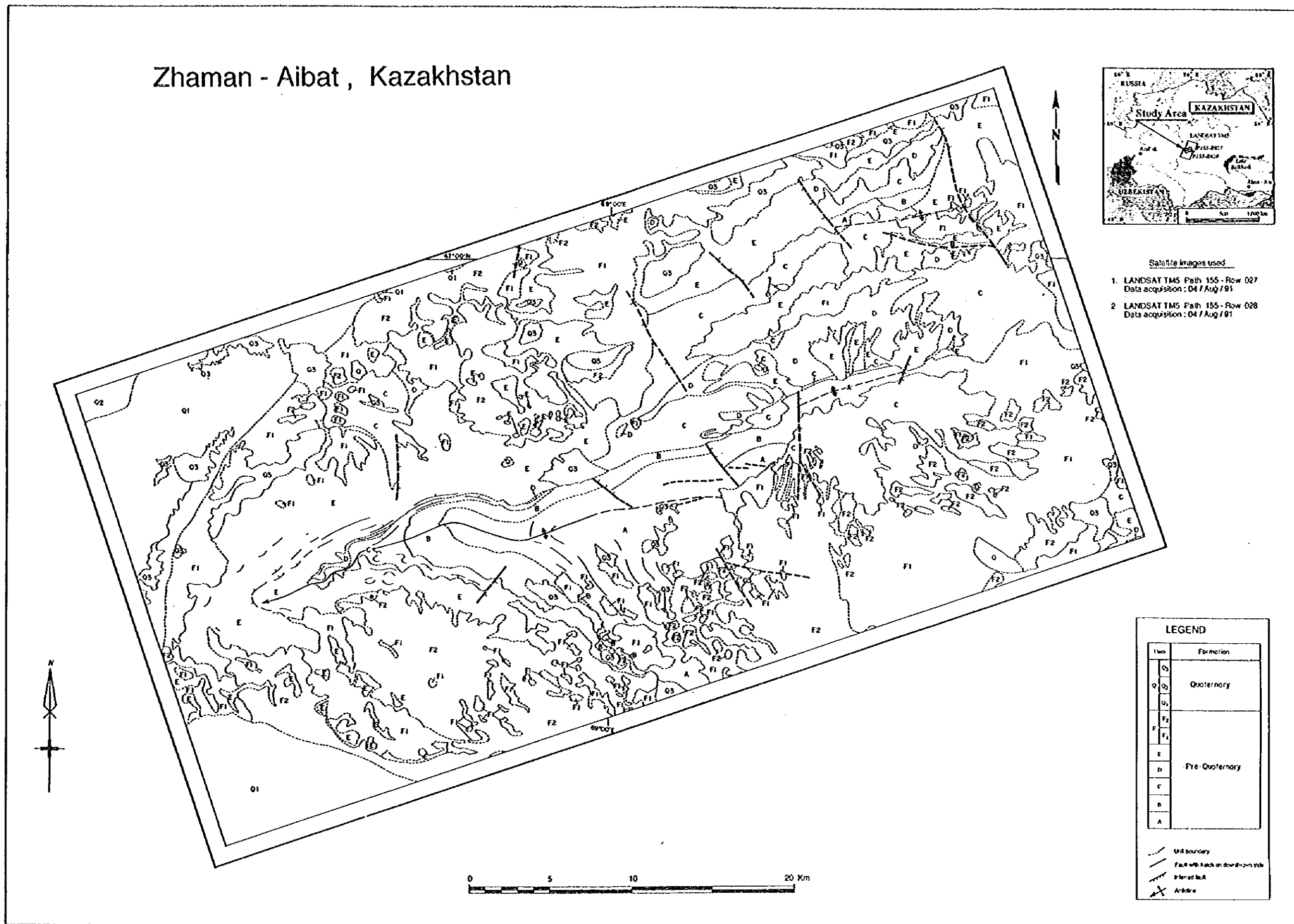


Fig. 2-4-3 Geological Classification of the Satellite Image in the Zhaman-Aibat Area





### 4-3-2 Results of Digital Image Processing

The Zhaman-Aibat area contains stratiform copper deposits related to weakly altered sedimentary rocks. In an attempt to identify this type of mineralization a spectral analysis was carried out with all band data. The method involved generation of color composite images and color density slice maps in order to distinguish alteration zones. The images and maps are composed of spectral or ratios of spectral bands.

A color ratio composite image (RGB; 5/7, 5/4, 3/1) is shown as extracted alteration zones in Fig. 2-4-4. Three processed color areas are associated with the Zhaman-Aibat horst anticline; a blue area spreads as a triangle-form to the west of the horst, a reddish purple area surrounds the horst in a semicircle, and the rest of the area is yellowish green. A processed blue area corresponds to geologic units A and B, that correspond to red sandstone in Carboniferous. The blue area identifies iron oxide and iron hydroxide that coincides with the "red sandstone". According to the fact that the red sandstone contains ores, the area of blue in the image is a valid target in peripheral sedimentary rocks in the survey area.

The reddish purple area corresponds to geologic unit Q3, which is made up of Quaternary sediments surrounding the Zhaman-Aibat horst anticline. Some of the reddish parts correspond to group of lakes which expand their areas during summer. It is difficult to make a judgement on the existence of clay minerals in the reddish area (band 7/5) without sufficient ground truth information. The yellowish green area corresponds to geologic units F1, F2 and Q1, which are widely distributed in the survey area. These rocks represent weathered layers of Quaternary and of Cretaceous age. It is believed that the yellowish color reflects alteration minerals in the weathered layer mixed with clay minerals and iron oxides. The color has some variability in lightness; F1 corresponds to the dark part, and Q1 to the bright part. In next year's study it is necessary to do a spectral analysis of rocks and to make a ground truth in geologic units.

### 4-3-3 Digital Images and a Geologic Units

Digital images were compared to geologic units from photographic geology (Table 2-4-2). The result is shown below.

An alteration zone was extracted as a color ratio composite of blue. This distribution corresponds to geologic units A and B. A similar alteration and rock character are inferred in the geologic units C and D. Unit D shows a characteristic color of yellow in false color images (RGB; 432 and 571). But the geological horizon of C and D are younger than the ore bearing horizon of red sandstone. Next year these units must be checked by ground truth surveys.

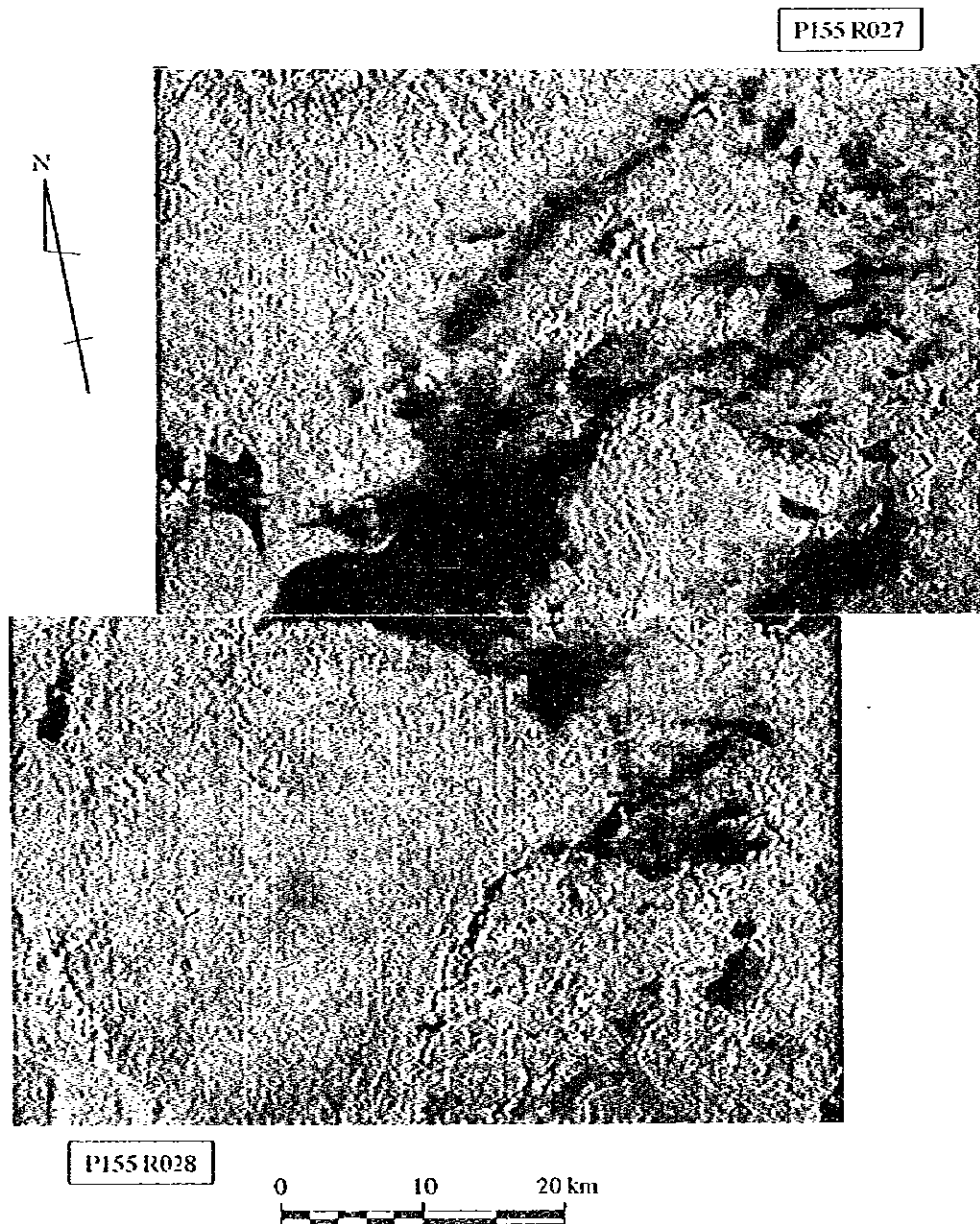
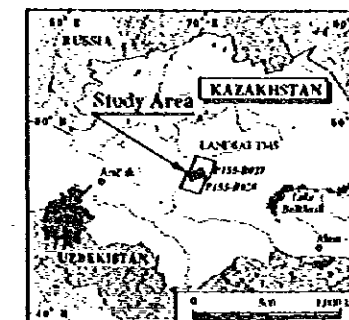


**Fig.2-4-4** Alteration Zone Extracted from the Satellite Image of the Zhaman-Albat Area

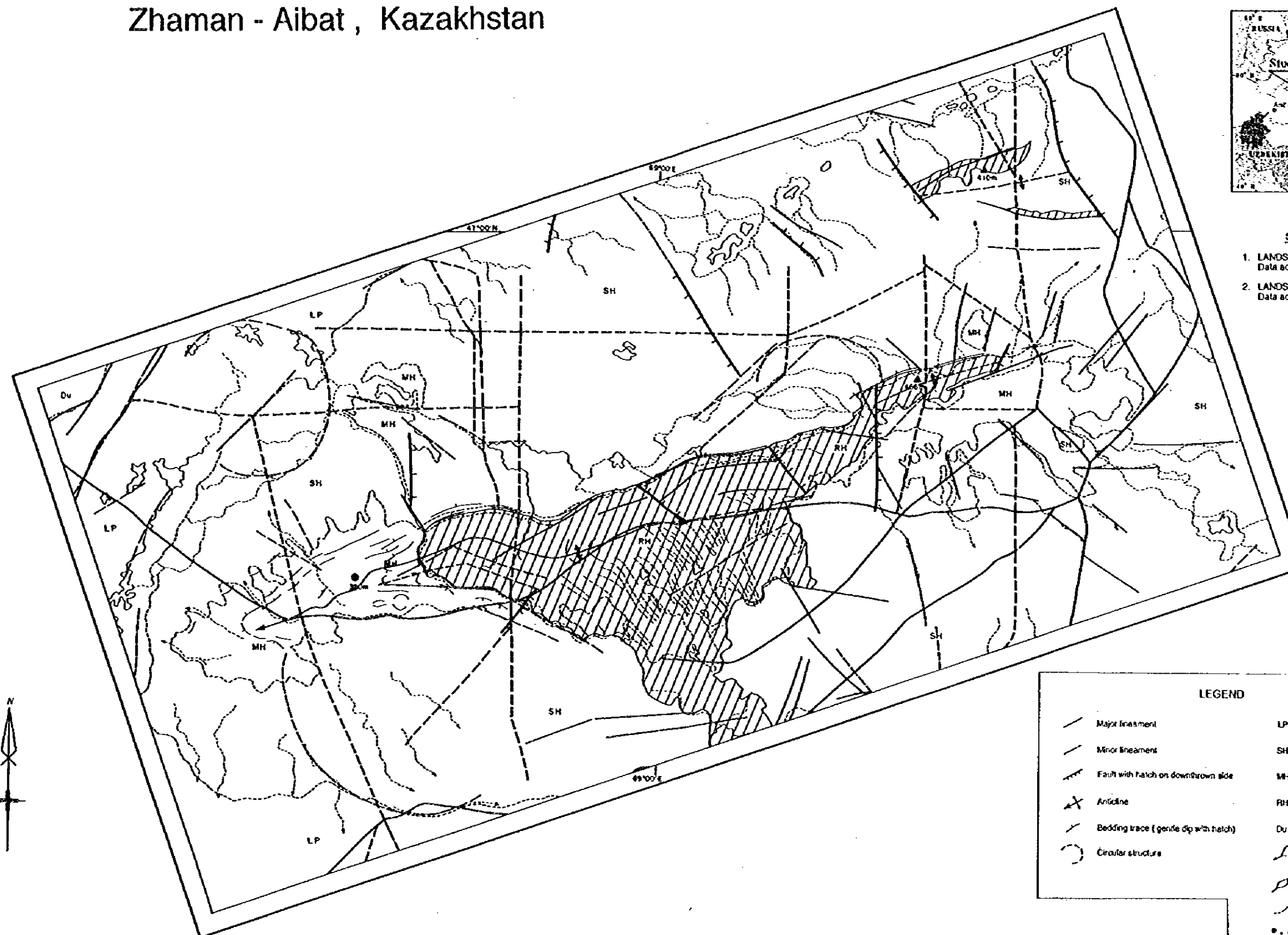


# Zhaman - Aibat , Kazakhstan



Satellite images used

1. LANDSAT TMS Path 155 - Row 027  
Data acquisition : 04 / Aug / 91
2. LANDSAT TMS Path 155 - Row 028  
Data acquisition : 04 / Aug / 91



LEGEND			
	Major lineament		LP Low plain
	Minor lineament		SH Smooth hill
	Fault with hatch on downthrown side		MH Moderate hill
	Anticline		RH Rough hill
	Bedding trace (gentle dip with hatch)		Du Dune
	Circular structure		Wadi, river
			Lake, swamp
			Unit boundary
			Point of elevation (m)
			Road
			Alteration Zone

Fig. 2-4-5 Interpretation Map of Satellite Image Analysis in the Zhaman - Aibat Area



**Table 2-4-2 Correlation between the Geologic Units and the Digital Image in the Zhama-Albat Area**

Geologic unit	Photo, RGB 541	False, RGB 5/7, 5/4, 3/1	False, RGB 432	False, RGB 571	Pseudo, RGB 7/5	Pseudo, RGB 4/3
Q3	white	reddish-violet	white (brown)	white (brown)	very low	very low
Q2	light-gray	reddish-violet	-	-	-	-
Q1	gray	yellowish-green	-	-	-	-
F2	dark gray	yellowish-green	grayish-green	yellowish-brown	middle	middle
F1	bluish-gray	yellowish-green	grayish-green	yellowish-brown	middle	middle
E	dark blue (white)	orange	grayish-green	dark brown	high	middle
D	yellow	-	yellow	yellow	high	middle
C	white	pink (white)	grayish-brown	-	high	middle
B	blue (orange)	dark blue	grayish-yellow	dark blue	high	middle
A	dark blue	dark blue	grayish-yellow	blue	high	middle

( ) partially